

Kriging: Beyond Matérn

Pulong Ma

Statistical and Applied Mathematical Sciences Institute and Duke University
79 T.W. Alexander Drive, P.O. Box 110207, Durham, NC 27709, USA
pulong.ma@duke.edu

and

Anindya Bhadra

Department of Statistics, Purdue University
250 N. University St., West Lafayette, IN 47907, USA
bhadra@purdue.edu

Abstract

The Matérn covariance function is a popular choice for prediction in spatial statistics and uncertainty quantification literature. A key benefit of the Matérn class is that it is possible to get precise control over the degree of differentiability of the process realizations. However, the Matérn class possesses exponentially decaying tails, and thus may not be suitable for modeling polynomially decaying dependence. This problem can be remedied using polynomial covariances; however one loses control over the degree of differentiability of the process realizations, in that the realizations using polynomial covariances are either infinitely differentiable or not differentiable at all. We construct a new family of covariance functions called the *Confluent Hypergeometric* (CH) class using a scale mixture representation of the Matérn class where one obtains the benefits of both Matérn and polynomial covariances. The resultant covariance contains two parameters: one controls the degree of differentiability near the origin and the other controls the tail heaviness, independently of each other. Using a spectral representation, we derive theoretical properties of this new covariance including equivalence measures and asymptotic behavior of the maximum likelihood estimators under infill asymptotics. The improved theoretical properties in predictive performance of this new covariance class are verified via extensive simulations. Application using NASA's Orbiting Carbon Observatory-2 satellite data confirms the advantage of this new covariance class over the Matérn class, especially in extrapolative settings.

Keywords: Equivalence measures; Gaussian process; Gaussian scale mixture; Polynomial dependence; XCO2.

1 Introduction

Kriging, a method for deriving the best spatial linear unbiased predictor in Gaussian process regression, is a term coined by Matheron (1963) in honor of the South African mining engineer D. G. Krige (Cressie, 1990). With origins in geostatistics, applications of kriging has permeated fields as diverse as spatial statistics (e.g., Banerjee et al., 2014; Berger et al., 2001; Cressie, 1993; Journel and Huijbregts, 1978; Matérn, 1960; Ripley, 1981; Stein, 1999), uncertainty quantification or UQ (e.g., Berger and Smith, 2019; Gu et al., 2018; Sacks et al., 1989; Santner et al., 2018) and machine learning (Williams and Rasmussen, 2006). Suppose $\{Z(\mathbf{s}) \in \mathbb{R} : \mathbf{s} \in \mathcal{D} \subset \mathbb{R}^d\}$ is a stochastic process

with a covariance function $\text{cov}(Z(\mathbf{s}), Z(\mathbf{s} + \mathbf{h})) = C(\mathbf{h})$ that is solely a function of the increment \mathbf{h} . Then $C(\cdot)$ is said to be second-order stationary (or weakly stationary). Further, if $C(\cdot)$ is a function of $\|\mathbf{h}\|$ with $\|\cdot\|$ denoting the Euclidean norm, then $C(\cdot)$ is called isotropic. If the process $Z(\cdot)$ possesses a constant mean function and a weakly stationary (resp. isotropic) covariance function, the process $Z(\cdot)$ is called weakly stationary (resp. isotropic). Further, $Z(\cdot)$ is a Gaussian process (GP) if every finite-dimensional realization $Z(\mathbf{s}_1), \dots, Z(\mathbf{s}_n)$ jointly follows a multivariate normal distribution for $\mathbf{s}_i \in \mathcal{D}$ and every n .

The Matérn covariance function (Matérn, 1960) has been widely used in spatial statistics due to its flexible local behavior and nice theoretical properties (see, e.g., Stein, 1999) with increasing popularity in the UQ and machine learning literature (Guttorp and Gneiting, 2006). The Matérn covariance function is of the form:

$$\mathcal{M}(h) = \sigma^2 \frac{2^{1-\nu}}{\Gamma(\nu)} \left(\frac{\sqrt{2\nu}}{\phi} h \right)^\nu \mathcal{K}_\nu \left(\frac{\sqrt{2\nu}}{\phi} h \right), \quad (1)$$

where $\sigma^2 > 0$ is the variance parameter, $\phi > 0$ is the range parameter, and $\nu > 0$ is the smoothness parameter that controls the differentiability of the associated random process. Here $\mathcal{K}_\nu(\cdot)$ is the modified Bessel function of the second kind that satisfies $\mathcal{K}_\nu(h) \asymp (\pi/(2h))^{1/2} \exp(-h)$ as $h \rightarrow \infty$, where $f(x) \asymp g(x)$ denotes $\lim_{x \rightarrow \infty} f(x)/g(x) = c \in (0, \infty)$. Further, we use the notation $f(x) \sim g(x)$ if $c = 1$. Thus, using this asymptotic expression of $\mathcal{K}_\nu(h)$ for large h from Section 6 of Barndorff-Nielsen et al. (1982), the behavior of the Matérn covariance function is given by:

$$\mathcal{M}(h) \asymp h^{\nu-1/2} \exp \left(-\frac{\sqrt{2\nu}}{\phi} h \right), \quad h \rightarrow \infty.$$

Eventually, the $\exp(-\sqrt{2\nu}h/\phi)$ term dominates, and the covariance decays exponentially for large h . This exponential decay may make it unsuitable for capturing polynomially decaying dependence. This problem with the Matérn covariance can be remedied by using covariance functions that decay polynomially, such as the generalized Wendland (Gneiting, 2002) and generalized Cauchy covariance functions (Gneiting, 2000; Gneiting and Schlather, 2004), but in using these polynomial covariance functions one loses a key benefit of the Matérn family: that of the degree of differentiability of the process realizations. Process realizations with a Matérn covariance function are exactly $\lfloor \nu \rfloor$ times differentiable, whereas the realizations with a generalized Cauchy covariance function are either non-differentiable (very rough) or infinitely differentiable (very smooth), without any middle ground (Stein, 2005). The generalized Wendland covariance family also has limited flexibility near the origin compared to the Matérn class and has compact support (Gneiting, 2002).

Stochastic processes with polynomial covariance are ubiquitous in many scientific disciplines including geophysics, meteorology, hydrology, astronomy, agriculture and engineering; see Beran

(1992) for a survey. In UQ studies, certain inputs may have little impact on output from a computer model, and these inputs are called *inert inputs*; see Chapter 7 of Santner et al. (2018) for detailed discussions. Power-law covariance functions can allow for large correlations among distant observations and hence are more suitable for modeling these inert inputs. Most often, computer model outputs can have different smoothness properties due to the behavior of the physical process to be modeled. Thus, power-law covariances with the possibility of controlling the differentiability of stochastic process realizations are very desirable for modeling such output.

In spatial statistics, polynomial covariances have been studied in a limited number of works (e.g., Gay and Heyde, 1990; Gneiting, 2000; Haslett and Raftery, 1989). In the rest of the paper, we focus on investigation of polynomial covariances in spatial settings. For spatial modeling, polynomial covariance can improve prediction accuracy over large missing regions. A covariance function with polynomially decaying tail can be useful to model highly correlated observations. As a motivating example, Figure 1 shows a 16-day repeat cycle of NASA’s Level 3 data product of the column-averaged carbon dioxide dry air mole fraction (XCO₂) at 0.25° and 0.25° collected from the Orbiting Carbon Observatory-2 (OCO-2) satellite. The XCO₂ data are collected over longitude bands and have large missing gaps between them. Predicting the true process over these large missing gaps based on a spatial process model is challenging. If the covariance function only allows exponentially decaying dependence, the predicted true process will be dominated by the mean function in the spatial process model with the covariance function having negligible impact over these large missing gaps. However, if the covariance function can model polynomially decaying dependence, the predicted true process over these missing gaps will carry more information from distant locations where observations are available, presumably resulting in better prediction. Thus, it is of fundamental and practical interest to develop a covariance function with polynomially decaying tails, without sacrificing the control over the smoothness behavior of the process realizations.

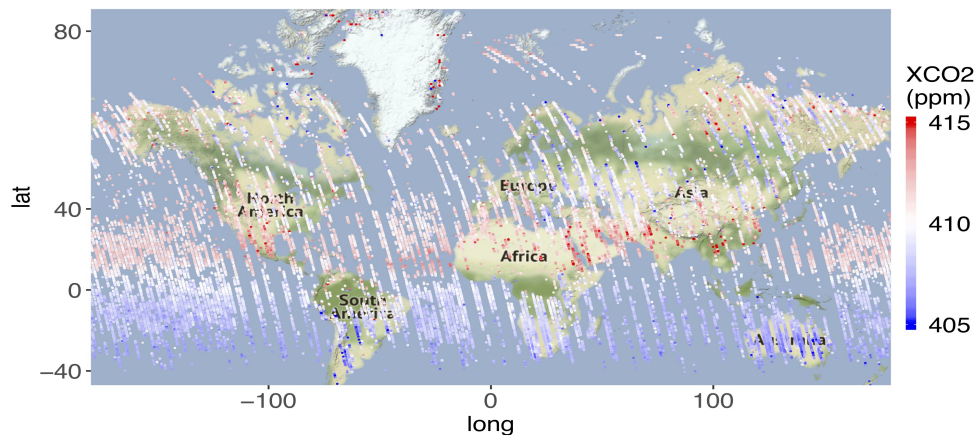


Fig. 1. XCO₂ data from June 1 to June 16, 2019. The units are parts per millions (ppm).

In this paper we propose a new family of covariance functions called the *Confluent Hypergeometric* (CH) class that bridges this gap between the Matérn covariance and polynomial co-

variances. The proposed covariance class is obtained by mixing the Matérn covariance over its range parameter ϕ . This is done by recognizing the Bessel function in the Matérn covariance function as proportional to the normalizing constant of the generalized inverse Gaussian distribution (Barndorff-Nielsen, 1977, 1978), which then allows analytically tractable calculations with respect to a range of choices for mixing densities, resulting in valid covariance functions with varied features. Apart from this technical innovation, the key benefit is that this mixing does not affect the origin behavior and thus allows one to retain the precise control over the smoothness of process realizations as in Matérn. However, the tail is inflated due to mixing, and, in fact, the mixing distribution can be chosen in a way so that the tail of the resultant covariance function displays regular variation, with precise control over the tail decay parameter α . A function $f(\cdot)$ is said to have a regularly decaying right tail with index α if it satisfies $f(x) \asymp x^{-\alpha}L(x)$ as $x \rightarrow \infty$ for some $\alpha > 0$ where $L(\cdot)$ is a slowly varying function at infinity with the property $\lim_{x \rightarrow \infty} L(tx)/L(x) = 1$ for all $t \in (0, \infty)$ (Bingham et al., 1989). Unlike a generalized Cauchy covariance function, this CH class is obtained without sacrificing the control over the degree of differentiability of the process, which is still controlled solely by ν , and the resulting process is still exactly $\lfloor \nu \rfloor$ times differentiable, independent of α . Moreover, regular variation is preserved under several commonly used transformations, such as sums or products. Thus, it is possible to exploit these properties of regular variation to derive CH covariances with similar features from the original covariance function that is obtained via a mixture of the Matérn class.

The rest of the paper is organized as follows. Section 2 begins with the construction of the proposed covariance function as a mixture of the Matérn covariance function over its range parameter. We verify that such construction indeed results in a valid covariance function. Moreover, we demonstrate that the behaviors of this covariance function near the origin and in the tails are characterized by two distinct parameters, which in turn control over the smoothness and the degree of polynomially decaying dependence, respectively. Section 3 presents the main theoretical results for the CH class. We first derive the spectral representation of this CH class and characterize its high-frequency behavior, and then show theoretical properties concerning equivalence classes under Gaussian measures and asymptotic normality of the maximum likelihood estimators. The resultant theory is extensively verified via simulations in Section 4. In Section 5, we use this CH covariance to analyze NASA’s OCO-2 data, and demonstrate better prediction results over the Matérn covariance. Section 6 concludes with some discussions for future investigations. All the technical proofs can be found in the Supplementary Material.

2 The CH Class as a Mixture of the Matérn Class

Our starting point in mixing over the range parameter ϕ in the Matérn covariance function is the correspondence between the form of the Matérn covariance function and the normalizing constant of the generalized inverse Gaussian distribution of Barndorff-Nielsen (1977). The generalized

inverse Gaussian distribution has density on $(0, \infty)$ given by:

$$\pi_{GIG}(x) = \frac{(a/b)^{p/2}}{2\mathcal{K}_p(\sqrt{ab})} x^{(p-1)} \exp\{-(ax + b/x)/2\}; \quad a, b > 0, p \in \mathbb{R}.$$

Thus,

$$\mathcal{K}_p(\sqrt{ab}) = \frac{1}{2} (a/b)^{p/2} \int_0^\infty x^{(p-1)} \exp\{-(ax + b/x)/2\} dx.$$

Take $a = \phi^{-2}, b = 2\nu h^2$ and $p = \nu$. Then we have the following representation of the Matérn covariance function with range parameter ϕ and smoothness parameter ν :

$$\begin{aligned} \mathcal{M}(h) &= \sigma^2 \frac{2^{1-\nu}}{\Gamma(\nu)} \left(\frac{\sqrt{2\nu}}{\phi} h \right)^\nu \mathcal{K}_\nu \left(\frac{\sqrt{2\nu}}{\phi} h \right) \\ &= \sigma^2 \frac{2^{1-\nu}}{\Gamma(\nu)} \left(\frac{\sqrt{2\nu} h}{\phi} \right)^\nu \frac{1}{2} \left(\frac{1}{\sqrt{2\nu} h \phi} \right)^\nu \int_0^\infty x^{(\nu-1)} \exp\{-(x/\phi^2 + 2\nu h^2/x)/2\} dx \\ &= \frac{\sigma^2}{2^\nu \phi^{2\nu} \Gamma(\nu)} \int_0^\infty x^{(\nu-1)} \exp\{-(x/\phi^2 + 2\nu h^2/x)/2\} dx. \end{aligned}$$

Thus, the mixture over ϕ^2 with respect to a mixing measure $G(\phi^2)$ on $(0, \infty)$ can be written as

$$\begin{aligned} C(h) &:= \int_0^\infty \mathcal{M}(h) dG(\phi^2) \\ &= \int_0^\infty \left[\frac{\sigma^2}{2^\nu \phi^{2\nu} \Gamma(\nu)} \int_0^\infty x^{(\nu-1)} \exp\{-(x/\phi^2 + 2\nu h^2/x)/2\} dx \right] dG(\phi^2) \\ &= \frac{\sigma^2}{2^\nu \Gamma(\nu)} \int_0^\infty x^{(\nu-1)} \left[\int_0^\infty \phi^{-2\nu} \exp\{-x/(2\phi^2)\} dG(\phi^2) \right] \exp(-\nu h^2/x) dx. \end{aligned} \tag{2}$$

The resultant covariance via this mixture is quite general with different choices for the mixing measure $G(\phi^2)$. When the mixing measure $G(\phi^2)$ admits a probability density function, say $\pi(\phi^2)$, the inner integral may be recognized as a mixture of gamma integrals (by change of variable $u = \phi^{-2}$), which is analytically tractable for many choices of $\pi(\phi^2)$; see for example the chapter on gamma integrals in Abramowitz and Stegun (1965). More importantly, as we show below, the mixing density $\pi(\phi^2)$ can be chosen to achieve precise control over certain features of the resulting covariance function.

THEOREM 1. *Let $X \sim \mathcal{IG}(a, b)$ denote an inverse gamma random variable using the shape–scale parameterization with density $\pi_{IG}(x) = \{b^a / \Gamma(a)\} x^{-a-1} \exp(-b/x)$; $a, b > 0$. Assume that $\phi^2 \sim \mathcal{IG}(\alpha, \beta/2)$ and that $\mathcal{M}(h)$ is the Matérn covariance function in Equation (1). Then $C(h) = \int_0^\infty \mathcal{M}(h) \pi(\phi^2) d\phi^2$ is a valid covariance function on \mathbb{R}^d with the following form:*

$$C(h) = \frac{\sigma^2 \beta^\alpha \Gamma(\nu + \alpha)}{\Gamma(\nu) \Gamma(\alpha)} \int_0^\infty x^{(\nu-1)} (x + \beta)^{-(\nu+\alpha)} \exp(-\nu h^2/x) dx, \tag{3}$$

where $\sigma^2 > 0$ is the variance parameter, $\alpha > 0$ is called the tail decay parameter, $\beta > 0$ is called the scale

parameter, and $\nu > 0$ is called the smoothness parameter.

REMARK 1. Our approach to constructing the CH covariance by mixing over ϕ^2 leads to a well-defined covariance class that can be used for Gaussian process modeling. The resulting covariance has four parameters and inference can be performed either via maximum likelihood or Bayesian approaches, although we solely focus on the former in the current work. This construction should not be confused with Bayesian spatial modeling where a standard practice is to put a prior on the spatial range parameter in the Matérn covariance. More importantly, the likelihood under the CH covariance is fundamentally different from the posterior that is proportional to the product of the likelihood under the Matérn covariance and the prior on the spatial range parameter, where the prior could either be discrete or inverse gamma.

REMARK 2. It is also worth noting that our construction yields a covariance that is fundamentally different from a finite sum of Matérn covariances where the range parameter is assigned a discrete prior, since the latter does not possess polynomially decaying dependence and is undesirable for modeling spatial data in practice due to costly computation and lack of practical motivation. Moreover, individual covariances in the finite sum are not identifiable.

REMARK 3. The Matérn covariance is sometimes parameterized differently. The mixing density can be chosen accordingly to arrive at results identical to ours. For instance, with parameterization of the Matérn class given in Stein (1999), a gamma mixing density with shape parameter α and rate parameter $\beta/2$ would lead to an alternative route to the same representation of the CH class. The limiting case of the Matérn class is the squared exponential (or Gaussian) covariance when its smoothness parameter ν goes to ∞ . In this case, mixing over the inverse gamma distribution in Theorem 1 yields the Cauchy covariance.

Having established in Theorem 1 the resultant mixture as a valid covariance function, one may take a closer look at its properties. To begin, although the final form of $C(h)$ involves an integral, and thus may not appear to be in closed form at a first glance, the situation is indeed not too different from that of Matérn, where the associated Bessel function is available in an algebraically closed form only for certain special cases; otherwise it is available as an integral. In addition, this representation of $C(h)$ is sufficient for numerically evaluating the covariance function as a function of h via either quadrature or Monte Carlo methods. Additionally, with a certain change of variable, the above integral can be identified as belonging to a certain class of special functions that can be computed efficiently. More precisely, we have the following elegant representation of the CH class, justifying its name.

COROLLARY 1. *The proposed covariance function in Equation (3) can also be represented in terms of the confluent hypergeometric function of the second kind:*

$$C(h) = \frac{\sigma^2 \Gamma(\nu + \alpha)}{\Gamma(\nu)} \mathcal{U}(\alpha, 1 - \nu, \nu h^2 / \beta), \quad (4)$$

where $\alpha > 0, \beta > 0$ and $\nu > 0$. We name the proposed covariance class as the Confluent Hypergeometric (CH) class after the confluent hypergeometric function.

Proof. By making the change of variable $x = \beta/t$, standard calculation yields that

$$C(h) = \frac{\sigma^2 \Gamma(\nu + \alpha)}{\Gamma(\nu) \Gamma(\alpha)} \int_0^\infty t^{\alpha-1} (t+1)^{-(\nu+\alpha)} \exp(-\nu h^2 t / \beta) dt.$$

Thus, the conclusion follows by recognizing the form of the confluent hypergeometric function of the second kind $\mathcal{U}(a, b, c)$ from Chapter 13.2 of Abramowitz and Stegun (1965). \square

Equation (4) provides a convenient way to evaluate the CH covariance function, since efficient numerical calculation of the confluent hypergeometric function is implemented in various libraries such as the GNU scientific library (Galassi et al., 2002) and softwares including R and MATLAB, facilitating its practical deployment. For certain special parameter values, the evaluation of the confluent hypergeometric function can be as easy as the Matérn class; see Chapter 13.6 of Abramowitz and Stegun (1965). Besides the computational convenience, the CH covariance function in Equation (3) also allows us to make precise statements concerning the origin and tail behaviors of the resultant mixture. The next theorem makes the origin and tail behaviors explicit.

THEOREM 2. *The CH class has the following two properties:*

- (a) **Origin behavior:** *The differentiability of the CH class is solely controlled by ν in the same way as the Matérn class given in Equation (1).*
- (b) **Tail behavior:** *$C(h) \sim \frac{\sigma^2 2^{\alpha-1} \Gamma(\nu+\alpha)}{(\nu/\beta)^\alpha \Gamma(\nu)} |h|^{-2\alpha} L(h^2)$ as $h \rightarrow \infty$, where $L(x)$ is a slowly varying function at ∞ of the form $L(x) = \{x/(x + \beta/(2\nu))\}^{\nu+\alpha}$.*

Theorem 2 indicates that process realizations generated by the CH covariance function are $\lfloor \nu \rfloor$ times differentiable in the mean-square sense. The local behavior of this CH covariance function is very flexible in the sense that the parameter ν can allow for any degree of differentiability of a weakly stationary process in the same way as the Matérn class. However, its tail behavior is quite different from that of the Matérn class, since the CH covariance has a polynomial tail that decays slower than the exponential tail in the Matérn covariance function. This is natural since mixture inflates the tails in general, and in our particular case, changes the exponential decay to a polynomial one. The rate of tail decay is controlled by the parameter α . Thus, the CH class is more suitable for modeling polynomially decaying dependence which any exponentially decaying covariance function fails to capture. Moreover, the control over the degree of smoothness of process realizations is not lost. Theorem 2 also establishes a very desirable property that the degrees of differentiability near origin and the rate of decay of the tail for the CH covariance are controlled by two different parameters, ν and α , independently of each other. Each of these parameters can allow any degrees of flexibility.

REMARK 4. Porcu and Stein (2012) point out that it is possible to obtain a covariance function with flexible origin behavior and polynomial tails by simply taking a sum of a Matérn and a Cauchy

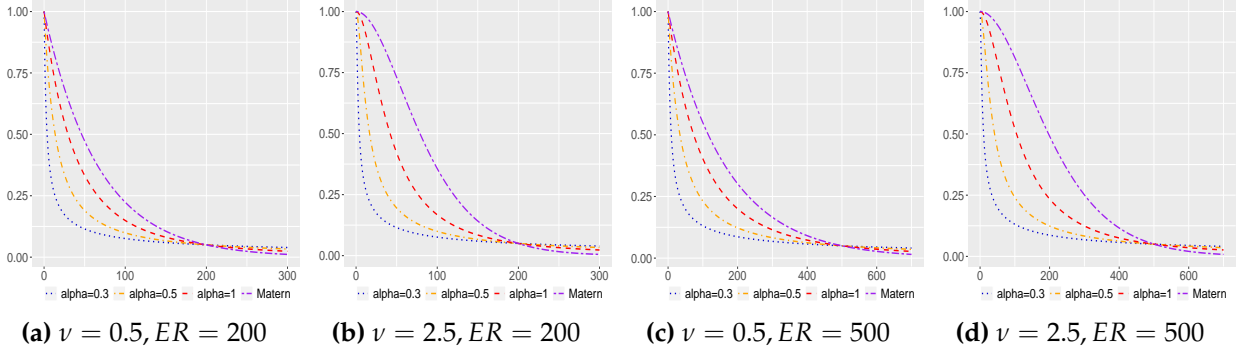


Fig. 2. Correlation functions for the CH class and the Matérn class. The panels (a) and (b) show the correlation functions with the effective range (ER) at 200. The panels (c) and (d) show the correlation functions with the effective range (ER) at 500. ER is defined as the distance at which correlation is approximately 0.05.

covariance, which is again a valid covariance function. There are three major difficulties in this approach compared to ours: (a) the individual covariances in such a finite sum are not identifiable and hence practical interpretation becomes difficult, although prediction may still be feasible, (b) this summed covariance has five parameters, hindering its practical use in both frequentist and Bayesian settings, since numerical optimization of the likelihood function is costly and judicious prior elicitation is likely to be difficult. In contrast, our covariance has four parameters, each of which has a well-defined role. Finally, (c) the microergodic parameter under such a summed covariance is not likely available in closed form, in contrast to ours, as derived later in Section 3.

EXAMPLE 1. To get a clear picture of the difference between the CH class and the Matérn class, we fix the effective range (ER) at 200 and 500, where ER is defined as the distance at which a correlation function has value approximately 0.05. For the CH class, we find the corresponding scale parameter β such that it has ER at 200 and 500 under different smoothness parameters $\nu \in \{0.5, 2.5\}$ and different tail decay parameters $\alpha \in \{0.3, 0.5, 1\}$. For the Matérn class, we find the corresponding range parameter ϕ such that it has ER at 200 and 500 under smoothness parameters $\nu \in \{0.5, 2.5\}$. These correlation functions are visualized in Figure 2. As the CH class has a polynomial tail, its correlation drops much faster than the Matérn class in order to reach the same correlation 0.05 at the same effective range. If α is smaller, the new correlation has a heavier tail, and hence it drops more quickly to reach the correlation 0.05 at the same effective range. After the effective range, the CH correlation with a smaller α decays slower than those with larger α . The faster decay of the tail in the Matérn class is indicated by the behavior after the ER. Corresponding 1-dimensional process realizations can be found in Section S.1 of the Supplementary Material.

3 Theoretical Properties of the CH Class

For an isotropic random field, the property of a covariance function can be characterized by its spectral density. The tail behavior of the spectral density can be used to derive properties of the theoretical results shown in later sections. The following proposition characterizes its tail behavior of the spectral density for the CH covariance function in Equation (3).

PROPOSITION 1 (Tail behavior of the spectral density). *The spectral density of the CH covariance function in Equation (3) admits the following tail behavior:*

$$f(\omega) \sim \frac{\sigma^2 2^{2\nu} \nu^\nu \Gamma(\nu + \alpha)}{\pi^{d/2} \beta^\nu \Gamma(\alpha)} \omega^{-(2\nu+d)} L(\omega^2), \quad \omega \rightarrow \infty,$$

where $L(x) = \{x/(x + \beta/(2\nu))\}^{\nu+d/2}$ is a slowly varying function at ∞ .

Recall that the spectral density of the Matérn class is proportional to $\omega^{-(2\nu+d)}$ for large ω . By mixing over the range parameter with an inverse gamma mixing density, the high-frequency behavior of the CH class differs from that of the Matérn class by a slowly varying function $L(\omega^2)$ up to a constant that does not depend any only frequency.

3.1 Equivalence Results

The equivalence of probability measures has important applications to statistical inferences on parameter estimation and prediction according to Zhang (2004). Let $\mathcal{P}_i, i = 1, 2$; be two probability measures corresponding to the spectral density f_i for stationary Gaussian process with mean zero in \mathbb{R}^d . If \mathcal{P}_1 is equivalent to \mathcal{P}_2 , then \mathcal{P}_1 cannot be correctly distinguished from \mathcal{P}_2 with \mathcal{P}_1 with probability 1 regardless of what is observed. Let $\{\mathcal{P}_\theta : \theta \in \Theta\}$ be a a sequence of distributions on the parameter space Θ and $\hat{\theta}_n$ be a sequence of estimators. Then $\hat{\theta}_n$ cannot be consistent estimators of θ for all $\theta \in \Theta$ under the infill asymptotics (or fixed domain asymptotics), where the domain is fixed (bounded) and the locations of observations get denser as the number of observations increases. The second application of equivalence measures concerns the asymptotic efficiency of predictors that is discussed in Section 3.3.

The tail behavior of the spectral densities in Proposition 1 can be used to check the equivalence of probability measures generated by stationary Gaussian random fields. The details of equivalence of Gaussian measures and the condition for equivalence can be found in Stein (1999) and references therein. Our first result on equivalence of two Gaussian measures under the CH class is given in Theorem 3.

THEOREM 3. *Let f_i be the spectral density of the covariance $C(h; \nu, \alpha_i, \beta_i, \sigma_i^2)$ for $i = 1, 2$. Then \mathcal{P}_1 and \mathcal{P}_2 are equivalent on the paths of $\{Z(\mathbf{s}) : \mathbf{s} \in \mathcal{D}\}$ for any bounded infinite set $\mathcal{D} \subset \mathbb{R}^d$ with $d = 1, 2, 3$ if and only if*

$$\frac{\sigma_1^2 \Gamma(\nu + \alpha_1)}{\beta_1^\nu \Gamma(\alpha_1)} = \frac{\sigma_2^2 \Gamma(\nu + \alpha_2)}{\beta_2^\nu \Gamma(\alpha_2)}. \quad (5)$$

An immediate consequence of Theorem 3 is that for fixed ν ; the tail decay parameter α , the scale parameter β and the variance parameter σ^2 cannot be estimated consistently under the infill asymptotics. Instead, the quantity $\sigma^2 \beta^{-\nu} \Gamma(\nu + \alpha) / \Gamma(\alpha)$ is consistently estimable and has been referred to as the *microergodic parameter*. We refer the readers to page 163 of Stein (1999) for the definition of microergodicity.

Theorem 3 gives the result on equivalence measures within the CH class. The CH can allow the same smoothness behavior as the Matérn class, but it has a polynomially decaying tail that is quite different from the Matérn class. One may ask whether there is an analogous result on the Gaussian measures under the CH class and the Matérn class. Theorem 4 provides an answer to this question.

THEOREM 4. *Let f_1 be the spectral density of the CH covariance $C(h; \nu, \alpha, \beta, \sigma_1^2)$ and f_2 be the spectral density of the Matérn covariance function $\mathcal{M}(h; \nu, \phi, \sigma_2^2)$. If*

$$\sigma_1^2 (\beta/2)^{-\nu} \Gamma(\nu + \alpha) / \Gamma(\alpha) = \sigma_2^2 \phi^{-2\nu}, \quad (6)$$

then \mathcal{P}_1 and \mathcal{P}_2 are equivalent on the paths of $\{Z(\mathbf{s}) : \mathbf{s} \in \mathcal{D}\}$ for any bounded infinite set $\mathcal{D} \subset \mathbb{R}^d$ with $d = 1, 2, 3$.

Theorem 4 gives the conditions under which the Gaussian measures under the CH class and the Matérn class are equivalent. If the condition in Equation (6) is satisfied, the Gaussian measure under the CH class cannot be distinguished from the Gaussian measure under the Matérn class, regardless of what is observed.

In Section 3.2, this microergodic parameter can be shown to be consistently estimated under infill asymptotics for a Gaussian process under the CH model with known ν . Moreover, one can show that this microergodic parameter converges to a normal distribution.

3.2 Asymptotic Normality

Let $\{Z(\mathbf{s}) : \mathbf{s} \in \mathcal{D}\}$ be a zero mean Gaussian process with the covariance function $C(h; \nu, \alpha, \beta, \sigma^2)$, where $\mathcal{D} \subset \mathbb{R}^d$ is a bounded subset of \mathbb{R}^d with $d = 1, 2, 3$. Let $\mathbf{Z}_n := (Z(\mathbf{s}_1), \dots, Z(\mathbf{s}_n))^\top$ be a partially observed realization of the process $Z(\cdot)$ at n distinct locations in \mathcal{D} , denoted by $\mathcal{D}_n := \{\mathbf{s}_1, \dots, \mathbf{s}_n\}$. Then the log-likelihood function is

$$\ell_n(\sigma^2, \boldsymbol{\theta}) = -\frac{1}{2} \left\{ n \log(2\pi\sigma^2) + \log |\mathbf{R}_n(\boldsymbol{\theta})| + \frac{1}{\sigma^2} \mathbf{Z}_n^\top \mathbf{R}_n^{-1}(\boldsymbol{\theta}) \mathbf{Z}_n \right\}, \quad (7)$$

where $\boldsymbol{\theta} := \{\alpha, \beta\}$ and $\mathbf{R}_n(\boldsymbol{\theta}) = [R(\|\mathbf{s}_i - \mathbf{s}_j\|; \boldsymbol{\theta})]_{i,j=1,\dots,n}$ is an $n \times n$ correlation matrix with the correlation function $R(h) := C(h) / \sigma^2$.

In what follows, ν is assumed to be known and fixed. Let $\hat{\sigma}_n^2$ and $\hat{\boldsymbol{\theta}}_n$ be the maximum likelihood estimators (MLE) for σ^2 and $\boldsymbol{\theta}$ by maximizing the log-likelihood function in Equation (7). To show the consistency and asymptotic results for the microergodic parameter, we first obtain an estimator

for σ^2 when θ is fixed: $\hat{\sigma}_n^2 = \mathbf{Z}_n^\top \mathbf{R}_n^{-1}(\theta) \mathbf{Z}_n / n$. Then, let $\hat{c}_n(\theta)$ be the maximum likelihood estimator of $c(\theta) := \sigma^2 \beta^{-\nu} \Gamma(\nu + \alpha) / \Gamma(\alpha)$, as a function of θ , given by

$$\hat{c}_n(\theta) = \frac{\hat{\sigma}_n^2 \Gamma(\nu + \alpha)}{\beta^\nu \Gamma(\alpha)} = \frac{\mathbf{Z}_n^\top \mathbf{R}_n^{-1}(\theta) \mathbf{Z}_n \Gamma(\nu + \alpha)}{n \beta^\nu \Gamma(\alpha)}.$$

We have the following results on the asymptotic properties of $\hat{c}_n(\theta)$ for various scenarios of α and β under the infill asymptotics.

THEOREM 5 (Asymptotics of the MLE). *Let \mathcal{D}_n be an increasing sequence of subsets of \mathcal{D} . Assume that $d/2 < \alpha_L < \alpha_U$ and $0 < \beta_L < \beta_U$. Let $\hat{c}_n(\alpha, \hat{\beta}_n)$ be the MLE of the microergodic parameter $c(\alpha_0, \beta_0)$ over $[\beta_L, \beta_U] \times (0, \infty)$ for any fixed $\alpha > 0$, $\hat{c}_n(\hat{\alpha}_n, \beta)$ be the MLE of the microergodic parameter $c(\alpha_0, \beta_0)$ over $[\alpha_L, \alpha_U] \times (0, \infty)$ for any fixed $\beta > 0$, and $\hat{c}_n(\hat{\alpha}_n, \hat{\beta}_n)$ be the MLE of the microergodic parameter $c(\alpha_0, \beta_0)$ over $[\alpha_L, \alpha_U] \times [\beta_L, \beta_U] \times (0, \infty)$. Then under $C(h; \nu, \alpha_0, \beta_0, \sigma_0^2)$, as $n \rightarrow \infty$, the following results can be established:*

- (a) $\hat{c}_n(\alpha, \hat{\beta}_n) \xrightarrow{a.s.} c(\theta_0)$ and $\sqrt{n} \{ \hat{c}_n(\alpha, \hat{\beta}_n) - c(\theta_0) \} \xrightarrow{\mathcal{L}} \mathcal{N}(0, 2[c(\theta_0)]^2)$ for any fixed $\alpha > d/2$.
- (b) $\hat{c}_n(\hat{\alpha}_n, \beta) \xrightarrow{a.s.} c(\theta_0)$ and $\sqrt{n} \{ \hat{c}_n(\hat{\alpha}_n, \beta) - c(\theta_0) \} \xrightarrow{\mathcal{L}} \mathcal{N}(0, 2[c(\theta_0)]^2)$ for any fixed $\beta > 0$.
- (c) $\hat{c}_n(\hat{\theta}_n) \xrightarrow{a.s.} c(\theta_0)$ and $\sqrt{n} \{ \hat{c}_n(\hat{\theta}_n) - c(\theta_0) \} \xrightarrow{\mathcal{L}} \mathcal{N}(0, 2[c(\theta_0)]^2)$.

The first two results of Theorem 5 imply that the microergodic parameter can be estimated consistently by fixing $\alpha > d/2$ or $\beta > 0$. In practice, fixing either α or β may be too restrictive for modeling spatial processes. We would expect that the finite sample prediction performance can be improved by jointly maximizing σ^2, α, β for the CH class.

The third result of Theorem 5 establishes that the microergodic parameter can be consistently estimated by jointly maximizing the log-likelihood (7) over α and β . However, the current result requires that $\alpha > d/2$. This means that the CH covariance cannot decay too slowly in its tail in order to establish the consistency result. Nevertheless, this result shows a significant improvement over existing asymptotic normality results for other types of polynomially decaying covariance functions. For instance, it was shown by Bevilacqua and Faouzi (2019) that the microergodic parameter in the generalized Cauchy class can be estimated consistently under infill asymptotics. However, their results assume that the parameter that controls the tail behavior is fixed. This is similar to the first result of Theorem 5. Unlike their results, a theoretical improvement in Theorem 5 is that the asymptotic results for the microergodic parameter $c(\theta)$ can be obtained for the joint estimation of all three parameters, including the parameter that controls the decay of the tail. We have performed extensive simulation studies to verify Theorem 5 in Section S.4 of the Supplementary Material.

3.3 Asymptotic Prediction Efficiency

This section is focused on prediction of Gaussian process at a new location $\mathbf{s}_0 \notin \mathcal{D}_n$. This problem has been studied extensively when an incorrect covariance model is used. Our focus here

is to show the asymptotic efficiency and asymptotically correct estimation of prediction variance in the context of the CH class. Stein (1988) shows that both of these two properties hold when the Gaussian measure under a misspecified covariance model is equivalent to the Gaussian measure under the true covariance model. In the case of the CH class, Theorem 3 gives the conditions for equivalence of two Gaussian measures in the light of the microergodic parameter $c(\boldsymbol{\theta}) = \sigma^2 \beta^{-\nu} \Gamma(\nu + \alpha) / \Gamma(\alpha)$.

Under the CH model $C(h; \nu, \alpha, \beta, \sigma^2)$, we define the best linear unbiased predictor for $Z(\mathbf{s}_0)$ to be

$$\hat{Z}_n(\boldsymbol{\theta}) = \mathbf{r}_n^\top(\boldsymbol{\theta}) \mathbf{R}_n^{-1}(\boldsymbol{\theta}) \mathbf{Z}_n, \quad (8)$$

where $\mathbf{r}_n(\boldsymbol{\theta}) := [R(\|\mathbf{s}_0 - \mathbf{s}_i\|; \boldsymbol{\theta}, \nu)]_{i=1, \dots, n}$ is an n -dimensional vector. This predictor depends only on α, β, ν . If the true covariance is $C(h; \nu, \alpha_0, \beta_0, \sigma_0^2)$, the mean squared error of the predictor in Equation (8) is given by $\text{Var}_{\nu, \boldsymbol{\theta}_0, \sigma_0^2} \{\hat{Z}_n(\boldsymbol{\theta}) - Z(\mathbf{s}_0)\} = \sigma_0^2 \{1 - 2\mathbf{r}_n^\top(\boldsymbol{\theta}) \mathbf{R}_n^{-1}(\boldsymbol{\theta}) \mathbf{r}_n(\boldsymbol{\theta}_0) + \mathbf{r}_n^\top(\boldsymbol{\theta}) \mathbf{R}_n^{-1}(\boldsymbol{\theta}) \mathbf{R}_n(\boldsymbol{\theta}_0) \mathbf{R}_n^{-1}(\boldsymbol{\theta}) \mathbf{r}_n(\boldsymbol{\theta})\}$. If $\boldsymbol{\theta} = \boldsymbol{\theta}_0$, i.e., $\alpha = \alpha_0$ and $\beta = \beta_0$, the above expression simplifies to

$$\text{Var}_{\nu, \boldsymbol{\theta}_0, \sigma_0^2} \{\hat{Z}_n(\boldsymbol{\theta}_0) - Z(\mathbf{s}_0)\} = \sigma_0^2 \left\{1 - \mathbf{r}_n^\top(\boldsymbol{\theta}_0) \mathbf{R}_n^{-1}(\boldsymbol{\theta}_0) \mathbf{r}_n(\boldsymbol{\theta}_0)\right\}. \quad (9)$$

If the true model is $\mathcal{M}(h; \nu, \phi, \sigma^2)$, analogous expressions can be derived for $\text{Var}_{\nu, \phi_0, \sigma_0^2} \{\hat{Z}_n(\boldsymbol{\theta}) - Z(\mathbf{s}_0)\}$.

Let $f_i(\omega), i = 1, 2$ be two spectral densities associated with two probability measures \mathcal{P}_i . The following results concern the asymptotic equivalence between the best linear predictor (BLP) under a misspecified probability measure \mathcal{P}_2 and the BLP under the true measure \mathcal{P}_1 .

THEOREM 6. Suppose that $\mathcal{P}_0, \mathcal{P}_1$ are two Gaussian probability measures defined by a zero mean Gaussian process with the CH class $C(h; \nu, \alpha_i, \beta_i, \sigma_i^2)$ for $i = 1, 2$ on \mathcal{D} . The following results hold true:

(a) As $n \rightarrow \infty$,

$$\frac{\text{Var}_{\nu, \boldsymbol{\theta}_0, \sigma_0^2} \{\hat{Z}_n(\boldsymbol{\theta}_1) - Z(\mathbf{s}_0)\}}{\text{Var}_{\nu, \boldsymbol{\theta}_0, \sigma_0^2} \{\hat{Z}_n(\boldsymbol{\theta}_0) - Z(\mathbf{s}_0)\}} \rightarrow 1.$$

(b) Moreover, if $\sigma_0^2 \beta_0^{-\nu} \Gamma(\nu + \alpha_0) / \Gamma(\alpha_0) = \sigma_1^2 \beta_1^{-\nu} \Gamma(\nu + \alpha_1) / \Gamma(\alpha_1)$, then as $n \rightarrow \infty$,

$$\frac{\text{Var}_{\nu, \boldsymbol{\theta}_1, \sigma_1^2} \{\hat{Z}_n(\boldsymbol{\theta}_1) - Z(\mathbf{s}_0)\}}{\text{Var}_{\nu, \boldsymbol{\theta}_0, \sigma_0^2} \{\hat{Z}_n(\boldsymbol{\theta}_1) - Z(\mathbf{s}_0)\}} \rightarrow 1.$$

(c) Let $\hat{\sigma}_n^2 = \mathbf{Z}_n^\top \mathbf{R}_n^{-1}(\boldsymbol{\theta}_1) \mathbf{Z}_n / n$. It follows that almost surely under \mathcal{P}_0 , as $n \rightarrow \infty$,

$$\frac{\text{Var}_{\nu, \boldsymbol{\theta}_1, \hat{\sigma}_n^2} \{\hat{Z}_n(\boldsymbol{\theta}_1) - Z(\mathbf{s}_0)\}}{\text{Var}_{\nu, \boldsymbol{\theta}_0, \sigma_0^2} \{\hat{Z}_n(\boldsymbol{\theta}_1) - Z(\mathbf{s}_0)\}} \rightarrow 1.$$

Part (a) of Theorem 6 implies that if the smoothness parameter ν is correctly specified, any values for α and β will result in asymptotically efficient predictors. The condition $\sigma_0^2 \beta_0^{-\nu} \Gamma(\nu + \alpha_0) / \Gamma(\alpha_0) = \sigma_1^2 \beta_1^{-\nu} \Gamma(\nu + \alpha_1) / \Gamma(\alpha_1)$ is not necessary for asymptotic efficiency, but it provides asymptotically correct estimate of the mean squared prediction error (MSPE). The quantity $\text{Var}_{\nu, \boldsymbol{\theta}_1, \sigma_1^2} \{\hat{Z}_n(\boldsymbol{\theta}_1) - Z(\mathbf{s}_0)\}$ is the MSPE for $\hat{Z}_n(\boldsymbol{\theta}_1)$ under the model $C(h; \nu, \alpha_1, \beta_1, \sigma_1^2)$, while the quantity

$\text{Var}_{\nu, \theta_0, \sigma_0^2} \{\hat{Z}_n(\theta_1) - Z(\mathbf{s}_0)\}$ is the true MSPE for $\hat{Z}_n(\theta_1)$ under the true model $C(h; \nu, \alpha_0, \beta_0, \sigma_0^2)$. In practice, it is common to estimate model parameters and then prediction is made by plugging in these estimates into Equations (8) and (9). Part (c) shows the same convergence results if θ is fixed at θ_1 , but σ^2 is estimated via maximum likelihood method.

One can conjecture that the result in Part (c) of Theorem 6 still holds if θ_1 is replaced by its maximum likelihood estimator, but its proof seems elusive. Theorem 6 demonstrates the asymptotic prediction efficiency for the CH class. The following results are established to show the asymptotic efficiency of the best linear predictor under the CH class when the true Gaussian measure is generated by a zero-mean Gaussian process under the Matérn class.

THEOREM 7. *Let \mathcal{P}_0 be the Gaussian probability measure defined by a zero mean Gaussian process with the Matérn covariance class $\mathcal{M}(h; \nu, \phi, \sigma_0^2)$ and \mathcal{P}_1 be the Gaussian probability measure defined by a zero mean Gaussian process with the CH class $C(h; \nu, \alpha, \beta, \sigma_1^2)$ on \mathcal{D} . If the condition in Equation (6) is satisfied, then it follows that under the Gaussian measure \mathcal{P}_0 , as $n \rightarrow \infty$,*

$$\frac{\text{Var}_{\nu, \alpha, \beta, \sigma_1^2} \{\hat{Z}_n(\alpha, \beta, \nu) - Z(\mathbf{s}_0)\}}{\text{Var}_{\nu, \phi, \sigma_0^2} \{\hat{Z}_n(\phi, \nu) - Z(\mathbf{s}_0)\}} \rightarrow 1,$$

for any fixed $\alpha > 0$ and $\beta > 0$.

A key consequence of Theorem 7 is that when a true Gaussian process is generated by the Matérn covariance model, the CH covariance model (3) can yield an asymptotically equivalent BLP. The practical implication is when the true model is generated from the Matérn class, the predictive performance under the CH class is indistinguishable from that under the Matérn class as the number of observations gets larger in a fixed domain.

4 Numerical Illustrations

In this section, we use simulated examples to study the properties of the CH class and compare with alternative covariance models. In what follows, we compare the CH model with the other two covariance models: the Matérn class and the generalized Cauchy class. The predictive performance is evaluated based on root mean-squared prediction errors (RMSPE), coverage probability of the 95% percentile confidence intervals (CVG), and the average length of the predictive confidence intervals (ALCI) at held-out locations.

The goal of this section is to study the finite sample predictive performance under the CH model in interpolative settings. Specifically, we consider three different cases, where the true covariance model is specified as the Matérn covariance (Case 1), the CH (Case 2) and the generalized Cauchy (GC) covariance (Case 3), respectively. The Matérn class is very flexible near origin and has an exponentially decaying tail, the CH class is also very flexible near origin but has a polynomially decaying tail, and the GC class is either non-differentiable or infinitely differentiable and

has a polynomially decaying tail. The GC covariance has the form $C(h) = \sigma^2 \{1 + (h/\phi)^\delta\}^{-\lambda/\delta}$, where $\sigma^2 > 0$ is the variance parameter, $\phi > 0$ is the range parameter, $\lambda \in (0, d]$ is the parameter controlling the degree of polynomial decay, and $\delta \in (0, 2]$ is the smoothness parameter. When $\delta \in (0, 2)$, the corresponding process realizations will be non-differentiable. When $\delta = 2$, it corresponds to the Cauchy covariance, whose process realizations will be infinitely differentiable. For each case, predictive performance is compared at held-out locations with estimated covariance structures.

We simulate data in the square domain $\mathcal{D} = [0, 2000] \times [0, 2000]$ from mean zero Gaussian processes with three different covariance function models: the Matérn covariance (Case 1), the CH class (Case 2), and the GC covariance (Case 3) for a variety of settings. We simulate $n = 500, 1000, 2000$ data points via maximin Latin hypercube design (Stein, 1987) for parameter estimation and evaluate predictive performance at 10-by-10 regular grid points in \mathcal{D} . We fix the variance parameter at 1 and consider moderate spatial dependence with effective range (ER) at 200 and 500 for the underlying true covariances. For each of these simulation settings, we use 30 different random number seeds to generate the realizations. We always choose the same smoothness parameter for the Matérn class and the CH class. For the GC covariance, we fix its smoothness parameter to be $\delta = \min\{2\nu, d\}$, since the Gaussian measure with the Matérn class is equivalent to that with the GC class under certain conditions when the smoothness parameter of the GC class is twice the smoothness parameter of the Matérn class (Bevilacqua and Faouzi, 2019). However, the smoothness parameter δ in the GC class cannot be greater than 2, otherwise the GC class is no longer a valid covariance function.

4.1 Case 1: Examples with the Matérn Class as Truth

In Case 1, we simulate Gaussian process realizations from the Matérn model with smoothness parameter ν fixed at 0.5 and 2.5 and effective range at 200 and 500. The parameters in each covariance model are estimated based on profile likelihood as described in Section 3.2. Figure 3 of the Supplementary Material shows the estimated covariance structures and summary of prediction results. Regardless of the smoothness behavior and strength of dependence in the underlying true process, there is no clear difference between the CH class and the Matérn class in terms of estimated covariance structures and prediction performance. In contrast, the estimated GC covariance structure only performs as accurately as the Matérn class when $\nu = 0.5$. When the process realizations are twice differentiable ($\nu = 2.5$), as expected, the GC class cannot mimic such behavior, and hence, yields worse estimates of the covariance structures and prediction results compared to both the Matérn class and the CH class. The CH covariance is able to capture the true covariance structure as implied by Theorem 7, although it is not as accurate as the estimated Matérn covariance. In terms of RMSPE, there is no clear difference between the estimates under the CH class and the estimates under the Matérn class. However, the CVG and ALCI based on the CH class are slightly larger than those based on the estimated Matérn covariance.

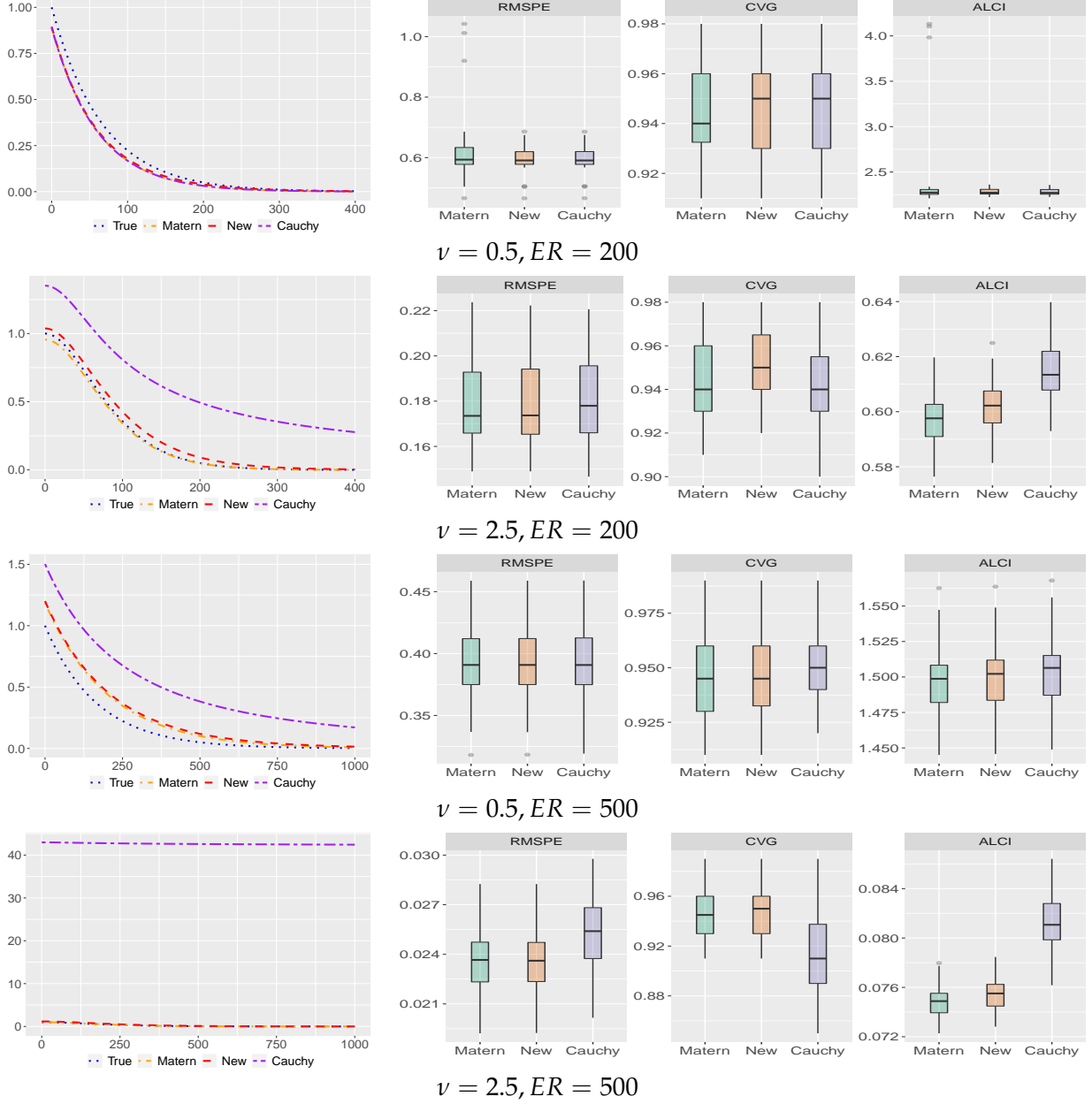


Fig. 3. Case 1: Comparison of predictive performance and estimated covariance structures when the true covariance is the Matérn class with 2000 observations. The predictive performance is evaluated at 10-by-10 regular grids in the square domain. These figures summarize the predictive measures based on RMSPE, CVG and ALCI under 30 simulated realizations.

4.2 Case 2: Examples with the CH Class as Truth

In Case 2, we simulate Gaussian process realizations from the CH covariance model with smoothness parameter ν fixed at 0.5 and 2.5, tail decay parameter fixed at 0.5, and effective range fixed at 200 and 500. Figure 4 of the Supplementary Material shows the estimated covariance structures and summary of prediction results. As expected, when the underlying true process is simulated

from a process with polynomially decaying dependence, the Matérn class cannot be expected to capture such behavior. The prediction results also indicate that the Matérn class performs much worse than the other two covariance models. When the underlying true process is not differentiable ($\nu = 0.5$), there is no clear difference between the estimates under the GC covariance structure and the estimates under the CH covariance structure. However, when the underlying true process is twice differentiable ($\nu = 2.5$), it is obvious that the estimates under the GC covariance structure is not as accurate as the estimates under the CH covariance structure. This makes sense because the GC class is either non-differentiable or infinitely differentiable. In terms of prediction performance, the CH covariance class performs better than the GC class in terms of coverage probability.

4.3 Case 3: Examples with the GC Class as Truth

In Case 3, we simulate Gaussian process realizations from the GC class with the smoothness parameter $\delta = 1$ and $\lambda = 1$ under ER=200 and 500. The corresponding process is non-differentiable and corresponds to the smoothness parameter $\nu = 0.5$ in both the Matérn class and the CH class. The parameter λ in the GC class is fixed at 1 so that it corresponds to the tail parameter $\alpha = 0.5$ in the CH class. We did not consider Gaussian process realizations that are infinitely differentiable, since such process realizations are unrealistic for environmental processes. Figure 5 of the Supplementary Material shows the estimated covariance structures and prediction results. As expected, the Matérn class performs much worse than the CH class and the GC class for the same reason as in Case 2. Between the CH class and the GC class, no difference is seen in terms of estimated covariance structures and predictive performances. This is not surprising, since the CH class has a tail decay parameter α that is able to capture the tail behavior in the GC class.

4.4 Simulation Examples with Other Scenarios

The results in the three cases above are based $n = 2000$ observations. In Section S.5.1 of the Supplementary Material, we provide results on exactly the same simulation settings with $n = 500$ and 1000. Similar conclusions can be drawn there. In addition, we also investigate the predictive performance when the covariance of the underlying true process is a product of individual covariance functions in Section S.5.2 of the Supplementary Material. The examples there show significant improvement of the CH class over the Matérn class and the GC class. In all these simulation examples, we found that the CH class is quite flexible in terms of capturing both the smoothness and the tail behavior. No matter which covariance structure (the Matérn class or the GC class) the true underlying process is generated from, the CH class is able to capture the underlying true covariance structure with satisfactory performance as implied by our theoretical developments. In contrast, the Matérn class is not able to capture the underlying true covariance structure with polynomially decaying dependence and the GC class is not able to capture the underlying true

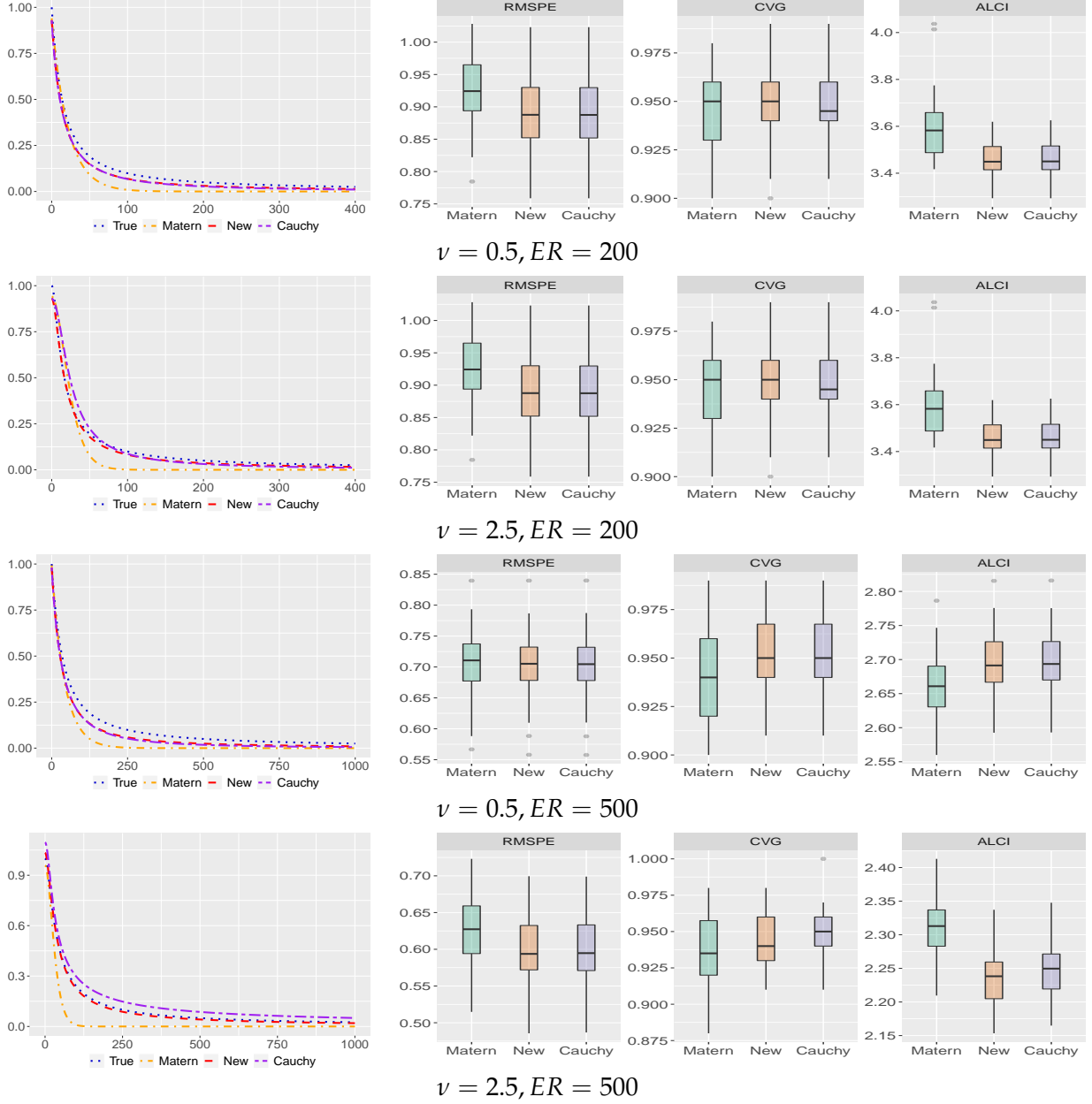


Fig. 4. Case 2: Comparison of predictive performance and estimated covariance structures when the true covariance is the CH class with 2000 observations. The predictive performance is evaluated at 10-by-10 regular grids in the square domain. These figures summarize the predictive measures based on RMSPE, CVG and ALCI under 30 simulated realizations.

covariance structure with different degrees of smoothness behaviors.

5 Application to the OCO-2 Data

In this section, the proposed CH class is used to model spatial data collected from NASA's Orbiting Carbon Observatory-2 (OCO-2) satellite and comparisons are made in kriging performances

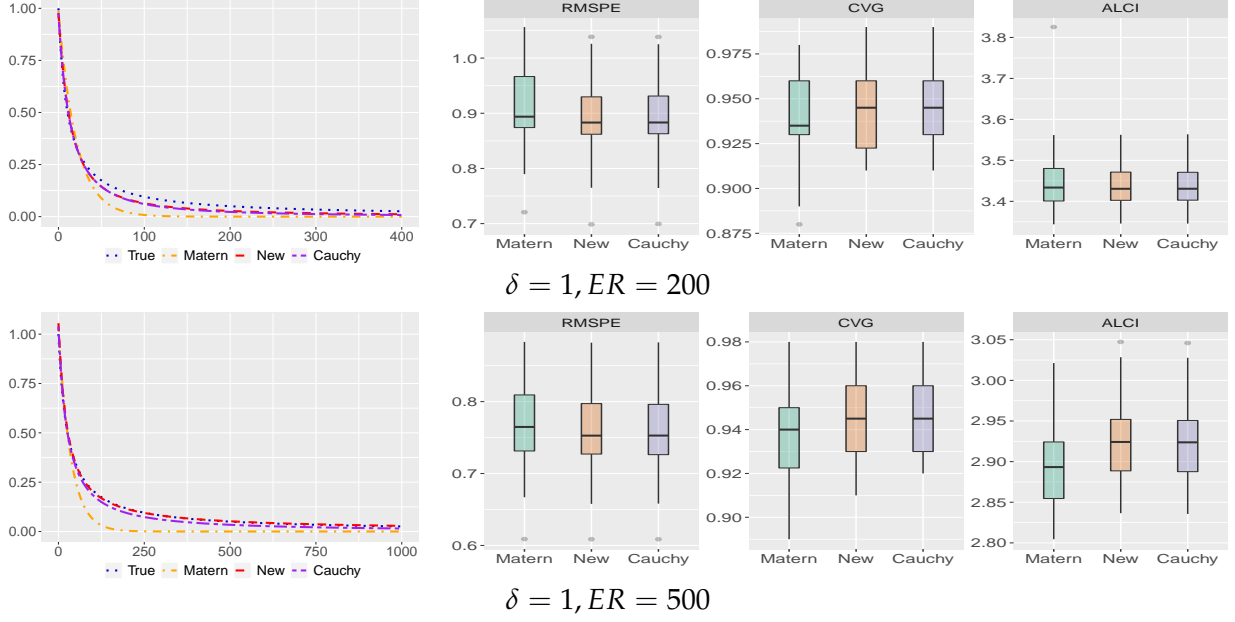


Fig. 5. Case 3: Comparison of predictive performance and estimated covariance structures when the true covariance is the GC class with 2000 observations. The predictive performance is evaluated at 10-by-10 regular grids in the square domain. These figures summarize the predictive measures based on RMSPE, CVG and ALCI under 30 simulated realizations.

with alternative covariances. The OCO-2 satellite is NASA’s first dedicated remote sensing earth satellite to study atmospheric carbon dioxide from space with the primary objective to estimate the global geographic distribution of CO₂ sources and sinks at Earth’s surface; see Cressie (2017); Wunch et al. (2011) for detailed discussions. The OCO-2 satellite carries three high-resolution grating spectrometers designed to measure the near-infrared absorption of reflected sunlight by carbon dioxide and molecular oxygen and orbits over a 16-day repeat cycle. In this application, we consider NASA’s Level 3 data product of the XCO₂ at $0.25^\circ \times 0.25^\circ$ spatial resolution over one repeat cycle from June 01 to June 16, 2019. These gridded data were processed based on Level 2 data product by the OCO-2 project at the Jet Propulsion Laboratory, California Technology, and obtained from the OCO-2 data archive maintained at the NASA Goddard Earth Science Data and Information Services Center. They can be downloaded at <https://co2.jpl.nasa.gov/#mission=OCO-2>.

This Level 3 data product consists of 43,698 measurements. We focus on the study region that covers the entire United States with longitudes between 140W and 50W and latitudes between 15N and 60N. This region includes 3,682 measurements; see panel (a) of Figure 6. These data points are very sparse in space. As the OCO-2 satellite has swath width 10.6 kilometers, large missing gaps can be observed between swaths. Predicting the underlying geophysical process based on data with such patterns requires the statistical model not only to interpolate in space (prediction near observed locations) but also to extrapolate in space (prediction away from observed locations).

Given the data $\mathbf{Z} := (Z(\mathbf{s}_1), \dots, Z(\mathbf{s}_n))^\top$, we assume a typical spatial process model:

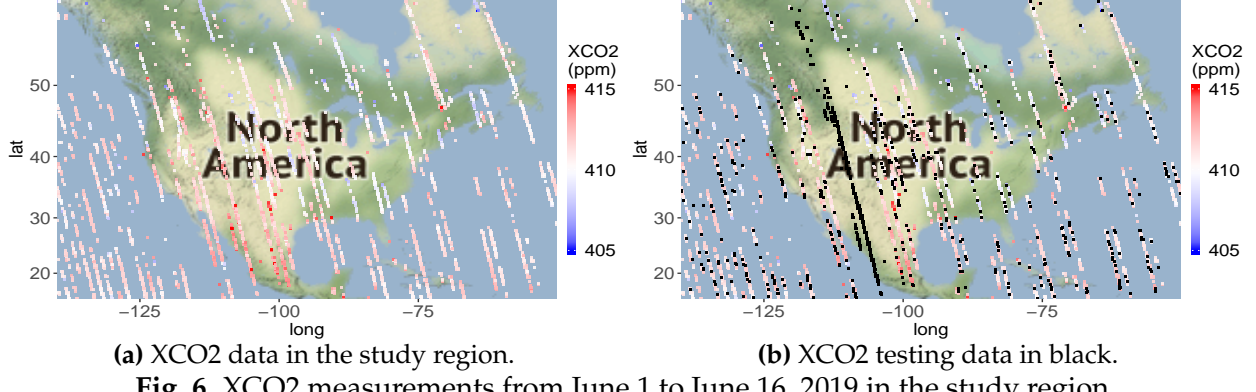


Fig. 6. XCO2 measurements from June 1 to June 16, 2019 in the study region.

$$Z(\mathbf{s}) = Y(\mathbf{s}) + \epsilon(\mathbf{s}), \quad \mathbf{s} \in \mathcal{D},$$

where $Y(\cdot)$ is assumed to be a Gaussian process with mean function $\mu(\cdot)$ and covariance function $C(\cdot, \cdot)$. The term $\epsilon(\cdot)$ is assumed to be a spatial white-noise process accounting for the nugget effect with $\text{var}(\epsilon(\mathbf{s})) = \tau^2 > 0$. The goal of this analysis is to predict the process $Y(\mathbf{s}_0)$ for any $\mathbf{s}_0 \in \mathcal{D}$ based on the data \mathbf{Z} . Exploratory analysis indicates no clear trend, so we assume a constant trend for the mean function $\mu(\mathbf{s}) = b$. For the covariance function $C(\cdot, \cdot)$, we assume the CH function model with parameters $\{\sigma^2, \alpha, \beta, \nu\}$, where the smoothness parameter ν is fixed at 0.5 and 1.5, which indicates the resulting process is non-differentiable or once differentiable, respectively.

To evaluate the performance of the CH class, we perform cross-validation and make comparisons with the Matérn class. The testing dataset consists of (1) a complete longitude band across the United States, which will be referred to as missing by design (MBD) and (2) randomly selected 15% of remaining XCO2 measurements, which will be referred to as missing at random (MAR). Panel (b) of Figure 6 highlights these testing data with black grid points. This dataset is used for evaluating out-of-sample predictive performance in an interpolative setting and an extrapolative setting. The remaining data points are used for parameter estimation under the Matérn covariance model and the CH covariance model. The parameters are estimated based on the restricted maximum likelihood (Harville, 1974). Table 1 shows the predictive measures and estimated nugget parameters. The CH model with the smoothness parameter $\nu = 0.5$ yields the smallest estimated nugget parameter among all the models. This suggests that the CH covariance model with $\nu = 0.5$ best captures the spatial dependence structure among all the models. The kriging predictions will shows more fine-scale or micro-scale variations, which are more desired for accurate spatial prediction. In an interpolative setting, the Matérn covariance model yields slightly smaller RMSPE and ALCI over randomly selected locations than the CH model, which indicates that the Matérn covariance model has slightly better interpolative prediction skill than the CH model. The empirical coverage probability is closer to the nominal value of 0.95 under the Matérn covariance model. In contrast, in an extrapolative setting, the CH model yields much smaller RMSPE and ALCI than the Matérn covariance model with indistinguishable empirical coverage probabilities, which indicates that the CH model has a better extrapolative prediction skill than the Matérn co-

variance model. These prediction results are not surprising, since the Matérn class can only model exponentially decaying dependence while the CH class can offer considerable benefits for extrapolative predictions while maintains the same interpolative prediction skill as the Matérn class. The difference in interpolative prediction performance between the CH class and the Matérn class is negligible, in part because the CH class can yield asymptotically equivalent best linear predictors as the Matérn class under conditions established in Theorem 7. Notice that the empirical coverage probabilities under all the models are less than the nominal coverage probability 0.95, this is partly because uncertainties due to parameter estimation are not accounted for in the predictive distribution. A fully Bayesian analysis may remedy this issue.

For other model parameters shown in Table S.4 of the Supplementary Material, we notice that the estimates of the regression parameters under the two different covariance models are the same. As expected, the estimated variance parameter (partial sill) is larger under the CH class than the one estimated under the Matérn class. Perhaps the most interesting parameter is the tail decay parameter in the CH class, which is estimated to be around 0.38. This clearly indicates that the underlying true process has a polynomially decaying dependence structure. As Gneiting (2013) points out, the Matérn class is positive definite on sphere only if $\nu \leq 0.5$ with great circle distance. To avoid this technical difficulty, we use chordal distance for modeling spatial data on sphere when $\nu > 0.5$, since Yadrenko (1983) points out that chordal distance can guarantee the positive definiteness of a covariance function on $\mathbb{S}^d \times \mathbb{S}^d$ when the original covariance function is positive definite on $\mathbb{R}^{d+1} \times \mathbb{R}^{d+1}$.

Table 1. Cross-validation results on the XCO2 data based on the Matérn covariance model and the CH covariance model. The measures in the first coordinate correspond to those based on MAR locations for interpolative prediction, and the measures in the second coordinate correspond to those based on MBD locations for extrapolative prediction.

	Matérn class		CH class	
	$\nu = 0.5$	$\nu = 1.5$	$\nu = 0.5$	$\nu = 1.5$
τ^2 (nugget)	0.0642	0.2215	0.0038	0.1478
RMSPE	0.672, 1.478	0.675, 1.599	0.676, 1.263	0.735, 1.227
CVG(95%)	0.952, 0.929	0.952, 0.951	0.944, 0.921	0.878, 0.937
ALCI(95%)	2.533, 5.095	2.536, 5.044	2.543, 4.722	2.098, 4.855

Next, we predict the process $Y(\cdot)$ at $0.25^\circ \times 0.25^\circ$ grid in the study region. The parameters are estimated based on all the data points under the CH class and the Matérn class with the smoothness parameter fixed at 0.5. In Figure S.9 of the Supplementary Material, we observe that the optimal kriging predictors over these grid points under the CH covariance model generally yield smaller values than those under the Matérn covariance function model in large missing gaps except for certain regions such as the Gulf of Mexico. More importantly, we also observe that the CH covariance model yields 10% to 20% smaller kriging standard errors than the Matérn covariance model in the observed spatial locations and contiguous missing regions. This indicates that

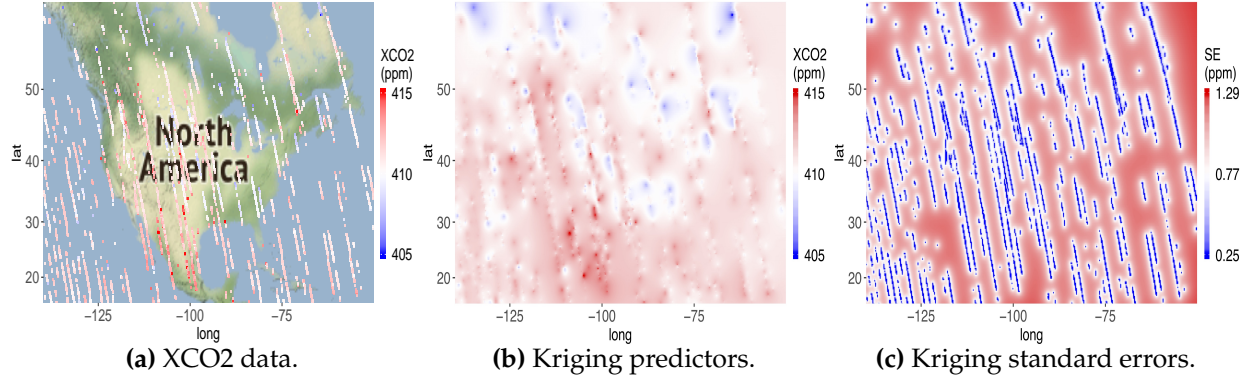


Fig. 7. XCO2 data and kriging predictions based on the CH model.

the CH covariance model has an advantage over the Matérn covariance in terms of in-sample prediction skills and in an extrapolative setting (such as large missing gaps). Prediction in an interpolative setting (such as locations near the observed locations) shows that the CH class yields indistinguishable (no more than 2%) kriging standard errors compared to the Matérn class. It is also very clear that the CH class is able to show lots of fine-scale variations in the kriging map, which is a desirable property for prediction accuracy. This is partly because the nugget parameter under the CH covariance is estimated to be much smaller than that under the Matérn covariance and partly because the polynomially decaying dependence exhibited in the CH class can better utilize information at both nearby locations and distant locations to infer such fine-scale variations. Finally, we show in Figure 7 the optimal kriging predictors and associated kriging standard errors at $0.25^\circ \times 0.25^\circ$ grid in the study region. These kriging maps help create a complete NASA Level 3 data product with associated uncertainties quantified in a statistically optimal way.

6 Concluding Remarks

This paper introduces a new class of covariance functions called the *Confluent Hypergeometric* class that can allow precise and simultaneous control of the origin and tail behaviors. Our approach in constructing the CH class is to mix over the range parameter of the Matérn class. As expected, the origin behavior of this CH class is as flexible as the Matérn class. The high-frequency behavior of the CH class is also similar to that of the Matérn class, since they differ by a slowly varying function up to a multiplicative constant. Unlike the Matérn class, however, this CH class has a polynomially decaying tail, which allows for modeling power-law stochastic processes.

The advantage of the CH class is examined in theory and numerical examples. Conditions for equivalence of two Gaussian measures based on the CH class are established. We derive the conditions on the asymptotic efficiency of kriging predictors based on an increasing number of observations in a bounded region when the CH covariance is misspecified. We also show that the CH class can yield an asymptotically efficient kriging predictor under the infill asymptotics framework when the true covariance belongs to the Matérn class. It is worth noting that the CH class

itself is valid and can allow any degrees of decaying tail, while the asymptotic results of the MLE for the microergodic parameters are proven for $\alpha > d/2$. Investigation of the similar theoretical result on the MLE is elusive for the case $\alpha \in (0, d/2]$. Extensive simulation results show that when the underlying true process is generated from either the Matérn covariance or the GC covariance, the CH covariance can yield as good predictive performance as the underlying true covariance model as shown in theory and simulation study. We also noticed in simulation study that the Matérn class gives worse performance than the CH class when the underlying true covariance has a polynomially decaying tail. In the real data analysis, we found the significant advantages of the CH class when used for prediction in an extrapolative setting while their difference in terms of interpolative prediction is indistinguishable as implied by our theoretical results. This feature is practically important for spatial modeling especially with large missing patterns. Future work along the theoretical side is to establish theoretical results of the CH class under the increasing domain asymptotics.

This paper mainly focuses on theoretical contributions and practical advantage of the CH class. Common challenges in spatial statistics include modeling large spatial data and spatial nonstationarity, which are often tackled based on the Matérn class in recent developments (e.g., Katzfuss and Guinness, 2020; Lindgren et al., 2011; Ma and Kang, 2020). The proposed CH class can be used as a substantially improved starting point over the Matérn class to develop more complicated covariance models to tackle these challenges. For instance, several extensions can be pursued. It is interesting to extend the proposed CH class for modeling dependence on sphere, space-time dependence, and/or multivariate dependence (e.g., Apanasovich et al., 2012; Ma and Kang, 2019; Ma et al., 2019). Prior elicitation for the CH class could be challenging. It is also interesting to develop objective priors such as reference prior to facilitate default Bayesian analysis for analyzing spatial data or computer experiments (Berger et al., 2001; Ma, 2019).

The CH class not only plays an important role in spatial statistics, but also is of particular interest in UQ. In the UQ community, a covariance function that is of a product form (e.g., Sacks et al., 1989; Santner et al., 2018) has been widely used to model dependence structures for computer model output to allow for different physical interpretations in each input dimension. The product form of this CH covariance can not only control the smoothness of the process realizations in each direction but also allow polynomially decaying dependence in each direction. The simulation example in Section S.5.2 of the Supplementary Material shows significant improvement of the CH class over the Matérn class and the GC class. Predicting real-world processes often relies on computer models whose output can have different smoothness properties and can be insensitive to certain inputs. This CH class can not only allow flexible control over the smoothness of the physical process of interest, but also allow near constant behavior along these inert inputs. Most often, predicting the real-world process involves extrapolation away from the original input space. The polynomially decaying dependence in combination with control over smoothness in the CH covariance should be useful in dealing with such challenging applications.

Supplementary Material

The Supplementary Material contains six parts: (1) 1-dimensional process realizations for the Matérn class and CH class, (2) two lemmas that are used to prove the main theorems, (3) technical proofs omitted in the main text, (4) simulation results that verify asymptotic normality, (5) additional simulation examples referenced in Section 4, and (6) parameter estimation results and figures referenced in Section 5.

Acknowledgements

The authors are grateful to Professor James O. Berger for commenting on an early draft of the manuscript. Bhadra gratefully acknowledges a visiting fellowship at the Statistical and Applied Mathematical Sciences Institute (SAMSI) where part of this research was conducted. This material is based upon work partially supported by the National Science Foundation under Grant DMS-1638521 to SAMSI.

References

- Abramowitz, M. and Stegun, I. A. (1965). *Handbook of mathematical functions: with formulas, graphs, and mathematical tables*, volume 55. Courier Corporation, North Chelmsford, MA.
- Apanasovich, T. V., Genton, M. G., and Sun, Y. (2012). A valid Matérn class of cross-covariance functions for multivariate random fields with any number of components. *Journal of the American Statistical Association* **107**, 180–193.
- Banerjee, S., Carlin, B. P., and Gelfand, A. E. (2014). *Hierarchical Modeling and Analysis for Spatial Data, Second Edition*. CRC Press, Boca Raton, FL.
- Barndorff-Nielsen, O. E. (1977). Exponentially decreasing distributions for the logarithm of particle size. *Royal Society of London Proceedings Series A* **353**, 401–419.
- Barndorff-Nielsen, O. E. (1978). Hyperbolic distributions and distributions on hyperbolae. *Scandinavian Journal of Statistics* **5**, 151–157.
- Barndorff-Nielsen, O. E., Kent, J. T., and Sørensen, M. (1982). Normal variance-mean mixtures and z distributions. *International Statistical Review* **50**, 145–159.
- Beran, J. (1992). Statistical methods for data with long-range dependence. *Statistical Science* **7**, 404–416.
- Berger, J. O., De Oliveira, V., and Sanso, B. (2001). Objective Bayesian analysis of spatially correlated data. *Journal of the American Statistical Association* **96**, 1361–1374.
- Berger, J. O. and Smith, L. A. (2019). On the statistical formalism of uncertainty quantification. *Annual Review of Statistics and Its Application* **6**, 433–460.

- Bevilacqua, M. and Faouzi, T. (2019). Estimation and prediction of Gaussian processes using generalized Cauchy covariance model under fixed domain asymptotics. *Electronic Journal of Statistics* **13**, 3025–3048.
- Bevilacqua, M., Faouzi, T., Furrer, R., and Porcu, E. (2019). Estimation and prediction using generalized Wendland covariance functions under fixed domain asymptotics. *The Annals of Statistics* **47**, 828–856.
- Bingham, N. H., Goldie, C. M., and Teugels, J. L. (1989). *Regular Variation*, volume 27 of *Encyclopedia of Mathematics and its Applications*. Cambridge University Press, Cambridge.
- Cressie, N. (1990). The origins of kriging. *Mathematical Geology* **22**, 239–252.
- Cressie, N. (1993). *Statistics for Spatial Data*. John Wiley & Sons, New York, revised edition.
- Cressie, N. (2017). Mission CO₂ntrol: A statistical scientist’s role in remote sensing of atmospheric carbon dioxide. *Journal of the American Statistical Association* **113**, 152–168.
- Galassi, M., Davies, J., Theiler, J., Gough, B., Jungman, G., Alken, P., Booth, M., Rossi, F., and Ulerich, R. (2002). *GNU scientific library*. Network Theory Limited.
- Gay, R. and Heyde, C. C. (1990). On a class of random field models which allows long range dependence. *Biometrika* **77**, 401–403.
- Gneiting, T. (2000). Power-law correlations, related models for long-range dependence and their simulation. *Journal of Applied Probability* **37**, 1104–1109.
- Gneiting, T. (2002). Compactly supported correlation functions. *Journal of Multivariate Analysis* **83**, 493–508.
- Gneiting, T. (2013). Strictly and non-strictly positive definite functions on spheres. *Bernoulli* **19**, 1327–1349.
- Gneiting, T. and Schlather, M. (2004). Stochastic models that separate fractal dimension and the hurst effect. *SIAM Review* **46**, 269–282.
- Gu, M., Wang, X., and Berger, J. O. (2018). Robust Gaussian stochastic process emulation. *The Annals of Statistics* **46**, 3038–3066.
- Guttorp, P. and Gneiting, T. (2006). Studies in the history of probability and statistics XLIX on the Matérn correlation family. *Biometrika* **93**, 989–995.
- Harville, D. A. (1974). Bayesian inference for variance components using only error contrasts. *Biometrika* **61**, 383–385.
- Haslett, J. and Raftery, A. E. (1989). Space-time modelling with long-memory dependence: Assessing Ireland’s wind power resource. *Journal of the Royal Statistical Society: Series C (Applied Statistics)* **38**, 1–50.
- Journel, A. G. and Huijbregts, C. J. (1978). *Mining Geostatistics*. Academic Press, Cambridge, MA.
- Katzfuss, M. and Guinness, J. (2020). A general framework for Vecchia approximations of Gaussian processes. *Statistical Science*. To appear.

- Kaufman, C. G. and Shaby, B. A. (2013). The role of the range parameter for estimation and prediction in geostatistics. *Biometrika* **100**, 473–484.
- Lindgren, F., Rue, H., and Lindström, J. (2011). An explicit link between Gaussian fields and Gaussian Markov random fields: the stochastic partial differential equation approach. *Journal of the Royal Statistical Society: Series B (Statistical Methodology)* **73**, 423–498.
- Ma, P. (2019). Objective Bayesian analysis of a cokriging model for hierarchical multifidelity codes. *arXiv:1910.10225*.
- Ma, P. and Kang, E. L. (2019). Spatio-temporal data fusion for massive sea surface temperature data from MODIS and AMSR-E instruments. *Environmetrics* **31**, 73.
- Ma, P. and Kang, E. L. (2020). A fused Gaussian process model for very large spatial data. *Journal of Computational and Graphical Statistics* **70**, 1–11. DOI:10.1080/10618600.2019.1704293.
- Ma, P., Konomi, B. A., and Kang, E. L. (2019). An additive approximate Gaussian process model for large spatio-temporal data. *Environmetrics* **30**, 1838.
- Matérn, B. (1960). *Spatial variation*, Meddelanden fran Statens Skogsforskningsinstitut, 49, 5. Second ed. (1986), Lecture Notes in Statistics 36, New York: Springer.
- Matheron, G. (1963). Principles of geostatistics. *Economic Geology* **58**, 1246–1266.
- Porcu, E. and Stein, M. L. (2012). On some local, global and regularity behaviour of some classes of covariance functions. In Porcu, E., Montero, J.-M., and Schlather, M., editors, *Advances and Challenges in Space-time Modelling of Natural Events*, pages 221–238, Berlin, Heidelberg. Springer Berlin Heidelberg.
- Ripley, B. (1981). *Spatial Statistics*. Wiley Series in Probability and Statistics. Wiley, New York.
- Sacks, J., Welch, W. J., Mitchell, T. J., and Wynn, H. P. (1989). Design and analysis of computer experiments. *Statistical Science* **4**, 409–423.
- Santner, T. J., Williams, B. J., and Notz, W. I. (2018). *The design and analysis of computer experiments; 2nd ed.* Springer series in statistics. Springer, New York.
- Schoenberg, I. J. (1938). Metric Spaces and Completely Monotone Functions. *Annals of Mathematics* **39**, 811–841.
- Stein, M. L. (1987). Large sample properties of simulations using Latin hypercube sampling. *Technometrics* **29**, 143–151.
- Stein, M. L. (1988). Asymptotically efficient prediction of a random field with a misspecified covariance function. *The Annals of Statistics* **16**, 55–63.
- Stein, M. L. (1993). A simple condition for asymptotic optimality of linear predictions of random fields. *Statistics & Probability Letters* **17**, 399 – 404.
- Stein, M. L. (1999). *Interpolation of Spatial Data: Some Theory for Kriging*. Springer Science & Business Media, New York, NY.
- Stein, M. L. (2005). Nonstationary spatial covariance functions. Unpublished Report. URL: https://cfpub.epa.gov/ncer_abstracts/index.cfm/fuseaction/display.files/fileID/14471.

- Stein, M. L. and Handcock, M. S. (1989). Some asymptotic properties of kriging when the covariance function is misspecified. *Mathematical Geology* **21**, 171–190.
- Wang, D. (2010). Fixed domain asymptotics and consistent estimation for Gaussian random field models in spatial statistics and computer experiments. PhD thesis, Department of Statistics and Applied Probability, National University of Singapore.
- Wang, D. and Loh, W.-L. (2011). On fixed-domain asymptotics and covariance tapering in Gaussian random field models. *Electronic Journal of Statistics* **5**, 238–269.
- Williams, C. K. and Rasmussen, C. E. (2006). *Gaussian processes for machine learning*. MIT press Cambridge, MA.
- Wunch, D., Toon, G. C., Blavier, J.-F. L., Washenfelder, R. A., Notholt, J., Connor, B. J., Griffith, D. W. T., Sherlock, V., and Wennberg, P. O. (2011). The total carbon column observing network. *Philosophical Transactions of the Royal Society A: Mathematical, Physical and Engineering Sciences* **369**, 2087–2112.
- Yadrenko, M. I. (1983). *Spectral theory of random fields*. Translation series in mathematics and engineering. Optimization Software, New York, NY. Transl. from the Russian.
- Yaglom, A. M. (1987). Correlation Theory of Stationary and Related Random Functions. *Springer Series in Statistics* .
- Zhang, H. (2004). Inconsistent estimation and asymptotically equal interpolations in model-based geostatistics. *Journal of the American Statistical Association* **99**, 250–261.

Web-based Supplementary Material for Kriging: Beyond Matérn

by

Pulong Ma

Statistical and Applied Mathematical Sciences Institute and Duke University

79 T.W. Alexander Drive, P.O. Box 110207, Durham, NC 27709, USA

pulong.ma@duke.edu

and

Anindya Bhadra

Department of Statistics, Purdue University

250 N. University St., West Lafayette, IN 47907, USA

bhadra@purdue.edu

This supplement contains six sections. Section S.1 shows 1-dimensional process realizations under different parameter values for the Matérn class and the CH class. Section S.2 shows some theoretical results that are used to prove main theorems in the main text. Section S.3 contains technical proofs that are omitted in the main text. Section S.4 contains simulation results that verify the theoretical results in Section 3. Section S.5 contains additional simulation results referenced in Section 4. Section S.6 contains parameter estimation results and figures referenced in Section 5.

S.1 1-D Process Realizations

In Figure S.1, we show the realizations from zero mean Gaussian processes with the CH class and the Matérn class under different parameter settings. When the distance is within the effective range, the Matérn covariance function results in more large correlations than the CH covariance function. This makes the process realizations from the Matérn class smoother even though both the Matérn class and the CH class are fixed at the same value for the smoothness parameter. For the CH class, if α has a smaller value, the corresponding correlation function has more small values within the effective range. This makes the process realizations under the CH class look rougher. As we expect, when the effective range and the tail decay parameter are fixed, the process realizations under the CH class look smoother for a larger value of the smoothness parameter.

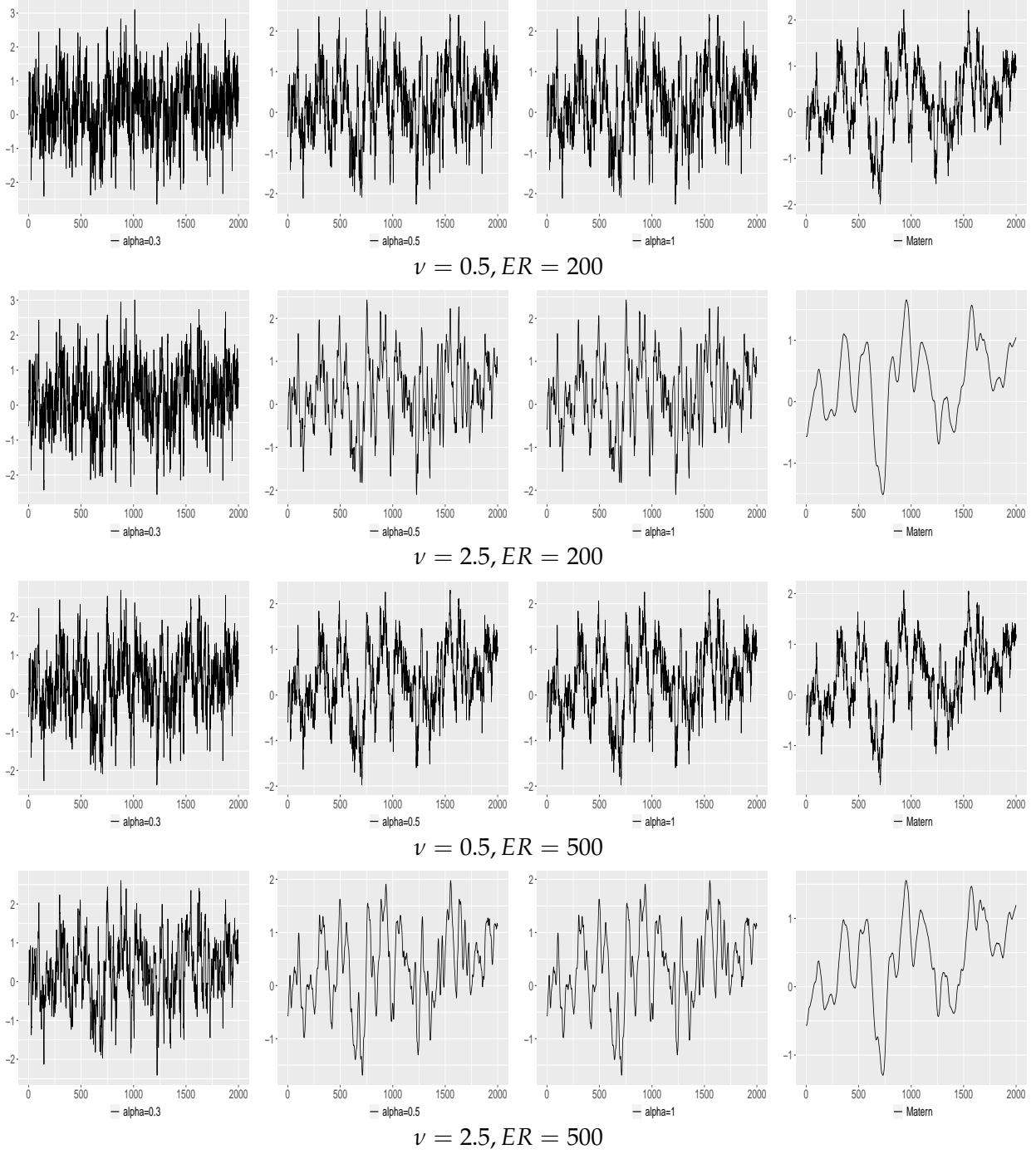


Fig. S.1. Realizations over 2000 regular grid points in the domain $[0, 2000]$ from zero mean Gaussian processes with the CH covariance model and the Matérn covariance model under different parameter settings. The realizations from the CH covariance are shown in the first three columns and those from the Matérn covariance are shown in the last column. For the first two rows, the effective range (ER) is fixed at 200. For the last two rows, the effective range is fixed at 500. ER is defined as the distance at which correlation is approximately 0.05.

S.2 Ancillary Results

The tail behavior of the spectral densities can be used to check the equivalence of probability measures generated by stationary Gaussian random fields. If for some $\lambda > 0$ and for some finite $c \in \mathbb{R}$, one has

$$0 < f_1(\omega)|\omega|^\lambda < \infty \quad \text{as} \quad |\omega| \rightarrow \infty, \quad \text{and} \quad (\text{S.1})$$

$$\int_{|\omega|>c} \left\{ \frac{f_1(\omega) - f_2(\omega)}{f_1(\omega)} \right\}^2 d\omega < \infty, \quad (\text{S.2})$$

then the two Gaussian measures \mathcal{P}_1 and \mathcal{P}_2 are equivalent. For isotropic Gaussian random fields, the condition in Equation (S.2) can be expressed as

$$\int_c^\infty \omega^{d-1} \left\{ \frac{f_1(\omega) - f_2(\omega)}{f_1(\omega)} \right\}^2 d\omega < \infty. \quad (\text{S.3})$$

The details of equivalence of Gaussian measures and the condition for equivalence can be found in a series of works (Stein, 1988, 1993, 1999; Stein and Handcock, 1989).

LEMMA 1. *Let \mathcal{D}_n be an increasing sequence of subsets of a bounded domain \mathcal{D} . Assume that ν is fixed. Then under $C(h; \nu, \alpha_0, \beta_0, \sigma_0^2)$, as $n \rightarrow \infty$, for any fixed $\alpha > 0$ and $\beta > 0$,*

$$(a) \quad \hat{c}_n(\boldsymbol{\theta}) \xrightarrow{a.s.} c(\boldsymbol{\theta}_0),$$

$$(b) \quad \sqrt{n} \{ \hat{c}_n(\boldsymbol{\theta}) - c(\boldsymbol{\theta}_0) \} \xrightarrow{\mathcal{L}} \mathcal{N}(0, 2[c(\boldsymbol{\theta}_0)]^2),$$

where $c(\boldsymbol{\theta}_0) = \sigma_0^2 \beta_0^{-\nu} \Gamma(\nu + \alpha_0) / \Gamma(\alpha_0)$.

Proof. The proof of the first statement follows from the same arguments as in the proof of Theorem 3 in Zhang (2004) and is omitted. For the proof of the second statement, we follow the arguments in Wang (2010); Wang and Loh (2011) and Bevilacqua et al. (2019) to prove the asymptotic normality of the MLE for the microergodic parameter. Without loss of generality, we assume $\mathcal{D} = [0, L]^d, 0 < L < \infty$ is a bounded subset of \mathbb{R}^d with $d = 1, 2, 3$. Let σ^2, α, β be positive constants such that $\sigma^2 \beta^{-\nu} \Gamma(\nu + \alpha) / \Gamma(\alpha) = \sigma_0^2 \beta_0^{-\nu} \Gamma(\nu + \alpha_0) / \Gamma(\alpha_0)$. Let $c(\boldsymbol{\theta}) = \sigma^2 \beta^{-\nu} \Gamma(\nu + \alpha) / \Gamma(\alpha)$ and $\hat{c}_n(\boldsymbol{\theta}) = \hat{\sigma}_n^2 \beta^{-\nu} \Gamma(\nu + \alpha) / \Gamma(\alpha)$. Then we have

$$\begin{aligned} \sqrt{n} \{ \hat{c}_n(\boldsymbol{\theta}) - c(\boldsymbol{\theta}_0) \} &= \frac{c(\boldsymbol{\theta}_0)}{\sqrt{n}} \left\{ \frac{1}{\sigma^2} \mathbf{Z}_n^\top \mathbf{R}_n^{-1}(\boldsymbol{\theta}) \mathbf{Z}_n - \frac{1}{\sigma_0^2} \mathbf{Z}_n^\top \mathbf{R}_n^{-1}(\boldsymbol{\theta}_0) \mathbf{Z}_n \right\} \\ &\quad + \frac{c(\boldsymbol{\theta}_0)}{\sqrt{n}} \left\{ \frac{1}{\sigma_0^2} \mathbf{Z}_n^\top \mathbf{R}_n^{-1}(\boldsymbol{\theta}_0) \mathbf{Z}_n - n \right\}. \end{aligned}$$

Under Gaussian measure \mathcal{P}_0 defined by the covariance function $C(h; \nu, \alpha_0, \beta_0, \sigma_0^2)$, we have

$$\mathbf{Z}_n^\top \mathbf{R}_n^{-1}(\boldsymbol{\theta}_0) \mathbf{Z}_n / \sigma_0^2 \sim \chi_n^2 \quad \text{and} \quad \frac{c(\boldsymbol{\theta}_0)}{\sqrt{n}} \left\{ \frac{1}{\sigma_0^2} \mathbf{Z}_n^\top \mathbf{R}_n^{-1}(\boldsymbol{\theta}_0) \mathbf{Z}_n - n \right\} \xrightarrow{\mathcal{L}} \mathcal{N}(0, 2[c(\boldsymbol{\theta}_0)]^2),$$

as $n \rightarrow \infty$. To prove the result, it suffices to show that

$$\frac{1}{\sqrt{n}} \left\{ \frac{1}{\sigma^2} \mathbf{Z}_n^\top \mathbf{R}_n^{-1}(\boldsymbol{\theta}) \mathbf{Z}_n - \frac{1}{\sigma_0^2} \mathbf{Z}_n^\top \mathbf{R}_n^{-1}(\boldsymbol{\theta}_0) \mathbf{Z}_n \right\} \xrightarrow{\mathbb{P}_0} 0, \quad \text{as } n \rightarrow \infty,$$

under Gaussian measure \mathcal{P}_0 . This is true if and only if for any $\epsilon > 0$,

$$\begin{aligned} & \mathbb{P}_0 \left(\frac{1}{\sqrt{n}} \left| \frac{1}{\sigma^2} \mathbf{Z}_n^\top \mathbf{R}_n^{-1}(\boldsymbol{\theta}) \mathbf{Z}_n - \frac{1}{\sigma_0^2} \mathbf{Z}_n^\top \mathbf{R}_n^{-1}(\boldsymbol{\theta}_0) \mathbf{Z}_n \right| > \epsilon \right) \\ &= \mathbb{P}_0 \left(\frac{1}{\sqrt{n}} \left| \sum_{k=1}^n (\lambda_{k,n}^{-1} - 1) Y_k^2 \right| > \epsilon \right) \rightarrow 0, \quad \text{as } n \rightarrow \infty, \end{aligned}$$

where $\mathbf{Y} := (Y_1, \dots, Y_n)^\top = \sigma_0^{-1} \mathbf{R}_n^{-1/2}(\boldsymbol{\theta}_0) \mathbf{Z}_n \sim \mathcal{N}_n(\mathbf{0}, \mathbf{I}_n)$ under \mathcal{P}_0 and $\lambda_{k,n}, k = 1, \dots, n$ are defined in the same way as in Wang (2010) and Wang and Loh (2011), satisfying

$$\sigma^2 [\sigma_0^{-1} \mathbf{R}_n^{-1/2}(\boldsymbol{\theta}_0)]^\top \mathbf{R}_n(\boldsymbol{\theta}) [\sigma_0^{-1} \mathbf{R}_n^{-1/2}(\boldsymbol{\theta}_0)] = \text{diag}\{\lambda_{k,n} : k = 1, \dots, n\}.$$

By the Markov's inequality,

$$\mathbb{P}_0 \left(\frac{1}{\sqrt{n}} \left| \sum_{k=1}^n (\lambda_{k,n}^{-1} - 1) Y_k^2 \right| > \epsilon \right) \leq \frac{1}{\epsilon \sqrt{n}} \sum_{k=1}^n |\lambda_{k,n}^{-1} - 1| \leq \frac{1}{\epsilon \sqrt{n}} \max_{1 \leq i \leq n} \sum_{k=1}^n \{\lambda_{i,n}^{-1}\} |\lambda_{k,n} - 1|.$$

The rest of the proof is to show that an upper bound of $\frac{1}{\epsilon \sqrt{n}} \max_{1 \leq i \leq n} \sum_{k=1}^n \{\lambda_{i,n}^{-1}\} |\lambda_{k,n} - 1|$ goes to 0 as $n \rightarrow \infty$. The detailed arguments follow similarly to the proof of Theorem 2 of Wang and Loh (2011) and the proof of Theorem 8 of Bevilacqua et al. (2019). The key difference is that the spectral density is not that of the Matérn class or Wendland class but that of the CH class. As the difference between the spectral density of the Matérn class and that of the CH lies in a multiplicative slowly varying function, all the proofs here should follow in a similar way as in the proof of Theorem 2 of Wang and Loh (2011). \square

Lemma 1 implies that the estimator $\hat{c}_n(\boldsymbol{\theta})$ of the microergodic parameter converges to the true

microergodic parameter, almost surely, when the number of observations tends to infinity in a fixed and bounded domain. This result holds true for any value of θ . As will be shown, if one replaces θ with its maximum likelihood estimator in $\hat{c}_n(\theta)$, this conclusion is true as well. The second statement of Lemma 1 indicates that $\hat{c}_n(\theta)$ converges to a normal distribution.

A key fact is that the above lemma holds true for arbitrarily fixed θ . A more practical situation is to estimate θ and σ^2 by maximizing the log-likelihood (7). For notational convenience, we use $c(\alpha, \beta)$ instead of $c(\theta)$ to denote the microergodic parameter when needed. We discuss three situations. In the first situation, we consider joint estimation of β and σ^2 for fixed α . The MLE of β will be denoted by $\hat{\beta}_n$, and the MLE of the microergodic parameter is $\hat{c}_n(\alpha, \hat{\beta}_n)$. In the second situation, we consider joint estimation of α and σ^2 for fixed β . The MLE of α will be denoted by $\hat{\alpha}_n$ and the MLE of the microergodic parameter is $\hat{c}_n(\hat{\alpha}_n, \beta)$. In the third situation, we consider joint estimation of all parameters α, β, σ^2 . Note that the MLEs of either α or β (or both) are typically computed numerically, since there is no closed-form expression. The following lemma is needed to prove the asymptotic behavior of $\hat{c}_n(\alpha, \hat{\beta}_n)$ and $\hat{c}_n(\hat{\alpha}_n, \beta)$ under infill asymptotics.

LEMMA 2. *Suppose that d is the dimension of the domain \mathcal{D} and \mathbf{Z}_n is a vector of n observations in \mathcal{D} . For any $\alpha_1 < \alpha_2$ and $\beta_1 < \beta_2$ with $\alpha_i \in [\alpha_L, \alpha_U]$ and $\beta_i \in [\beta_L, \beta_U]$, $i = 1, 2$, where $\alpha_L > d/2$ and $\beta_L > 0$, we have the following results:*

- (a) $\hat{c}_n(\alpha, \beta_1) \leq \hat{c}_n(\alpha, \beta_2)$ for any fixed $\alpha > d/2$.
- (b) $\hat{c}_n(\alpha_1, \beta) \geq \hat{c}_n(\alpha_2, \beta)$ for any fixed $\beta > 0$.

Proof. The difference

$$\hat{c}_n(\theta_1) - \hat{c}_n(\theta_2) = \mathbf{Z}_n^\top \left\{ \frac{\Gamma(\nu + \alpha_1)}{\beta_1^\nu \Gamma(\alpha_1)} \mathbf{R}_n^{-1}(\theta_1) - \frac{\beta_2^\nu \Gamma(\nu + \alpha_2)}{\beta_2^\nu \Gamma(\alpha_2)} \mathbf{R}_n^{-1}(\theta_2) \right\} \mathbf{Z}_n / n$$

is nonnegative for any \mathbf{Z}_n if the matrix $\mathbf{A} := \frac{\Gamma(\nu + \alpha_1)}{\beta_1^\nu \Gamma(\alpha_1)} \mathbf{R}_n^{-1}(\theta_1) - \frac{\Gamma(\nu + \alpha_2)}{\beta_2^\nu \Gamma(\alpha_2)} \mathbf{R}_n^{-1}(\theta_2)$ is positive semidefinite. Notice that \mathbf{A} is positive semidefinite if and only if $\mathbf{B} := \frac{\beta_2^\nu \Gamma(\alpha_2)}{\Gamma(\nu + \alpha_2)} \mathbf{R}_n(\theta_2) - \frac{\beta_1^\nu \Gamma(\alpha_1)}{\Gamma(\nu + \alpha_1)} \mathbf{R}_n(\theta_1)$ is positive semidefinite. The entries of \mathbf{B} can be expressed in terms of a function $K_B : \mathbb{R}^d \rightarrow \mathbb{R}$, with

$$B_{ij} = K_B(\mathbf{s}_i - \mathbf{s}_j) = \frac{\beta_2^\nu \Gamma(\alpha_2)}{\Gamma(\nu + \alpha_2)} R(\|\mathbf{s}_i - \mathbf{s}_j\|; \alpha_2, \beta_2, \nu) - \frac{\beta_1^\nu \Gamma(\alpha_1)}{\Gamma(\nu + \alpha_1)} R(\|\mathbf{s}_i - \mathbf{s}_j\|; \alpha_1, \beta_1, \nu),$$

and the matrix \mathbf{B} is positive semidefinite if K_B is a positive definite function. Define its Fourier

transform by

$$\begin{aligned}
f_B(\omega) &= \frac{1}{(2\pi)^d} \int_{\mathbb{R}^d} \exp\{-i\omega^\top x\} K_B(x) dx \\
&= \frac{\beta_2^\nu \Gamma(\alpha_2)}{\Gamma(\nu + \alpha_2)} \left\{ \frac{1}{(2\pi)^d} \int_{\mathbb{R}^d} \exp\{-i\omega^\top x\} R(x; \alpha_2, \beta_2, \nu) dx \right\} \\
&\quad - \frac{\beta_1^\nu \Gamma(\alpha_1)}{\Gamma(\nu + \alpha_1)} \left\{ \frac{1}{(2\pi)^d} \int_{\mathbb{R}^d} \exp\{-i\omega^\top x\} R(x; \alpha_1, \beta_1, \nu) dx \right\}.
\end{aligned}$$

The integrals in $f_B(\omega)$ are finite for $\alpha_1, \alpha_2 > d/2$. Let $g(\omega)$ be the spectral density of the CH correlation function with parameters α, β, ν :

$$\begin{aligned}
g(\omega) &:= \frac{1}{(2\pi)^d} \int_{\mathbb{R}^d} \exp\{-i\omega^\top x\} R(x; \alpha, \beta, \nu) dx \\
&= \frac{2^{2\nu} \nu^\nu}{\pi^{d/2} \beta^\nu \Gamma(\alpha)} \int_0^\infty \{4\nu/(\beta t) + \|\omega\|^2\}^{-(\nu+d/2)} t^{-(\nu+\alpha+1)} \exp\{-1/t\} dt.
\end{aligned}$$

Thus, K_B is positive definite if f_B is positive for all ω . Notice that f_B is given by

$$\begin{aligned}
f_B(\omega) &= \frac{(4\nu)^\nu}{\pi^{d/2} \Gamma(\nu + \alpha_2)} \int_0^\infty \{4\nu/(\beta_2 t) + \|\omega\|^2\}^{-(\nu+d/2)} t^{-(\nu+\alpha_2+1)} \exp\{-1/t\} dt \\
&\quad - \frac{(4\nu)^\nu}{\pi^{d/2} \Gamma(\nu + \alpha_1)} \int_0^\infty \{4\nu/(\beta_1 t) + \|\omega\|^2\}^{-(\nu+d/2)} t^{-(\nu+\alpha_1+1)} \exp\{-1/t\} dt.
\end{aligned}$$

It is straightforward to check that when $\alpha := \alpha_1 = \alpha_2 > d/2$,

$$\beta_1 < \beta_2 \implies f_B(\omega) > 0 \quad \text{for all } \omega.$$

Thus, if $\beta_1 < \beta_2$, then $\hat{c}_n(\alpha, \beta_1) \leq \hat{c}_n(\alpha, \beta_2)$.

The proof of the second statement is as follows. Note that $f_B(\omega)$ can be expressed as $f_B(\omega) = \{(4\nu)^\nu / \pi^{d/2}\} (I(\alpha_2) - I(\alpha_1))$, where

$$\begin{aligned}
I(\alpha) &:= \int_0^\infty \frac{1}{\Gamma(\nu + \alpha)} \{4\nu/(\beta t) + \|\omega\|^2\}^{-(\nu+d/2)} t^{-(\nu+\alpha+1)} \exp\{-1/t\} dt \\
&= \int_0^\infty \frac{u^{\nu+\alpha-1}}{\Gamma(\nu + \alpha)} \exp\{-u\} (4\nu u/\beta + \|\omega\|^2)^{-(\nu+d/2)} du \\
&= E_U (4\nu u/\beta + \|\omega\|^2)^{-(\nu+d/2)},
\end{aligned}$$

with $U \sim \text{Gamma}(\nu + \alpha, 1)$. This expectation is finite if $\alpha > d/2$. Suppose that $\alpha_1 < \alpha_2$ and $\beta := \beta_1 = \beta_2$. To show $f_B(\omega)$ is negative for all ω , it suffices to show that $I(\alpha_2) - I(\alpha_1) \leq 0$. Let $U_1 \sim \text{Gamma}(\nu + \alpha_1, 1)$ and $U_2 \sim \text{Gamma}(\nu + \alpha_2, 1)$. Then $U_2 \stackrel{\mathcal{L}}{=} U_1 + U_0$, where $U_0 \sim \text{Gamma}(\alpha_2 - \alpha_1, 1)$ and U_0 is independent of U_1 . Thus, the quantity $I(\alpha_2)$ can be upper bounded by $I(\alpha_1)$, since,

$$\begin{aligned} I(\alpha_2) &= E_{U_1, U_0} \left\{ \frac{4\nu}{\beta} (U_1 + U_0) + \|\omega\|^2 \right\}^{-(\nu+d/2)} \\ &= E_{U_1, U_0} \left\{ \frac{4\nu}{\beta} U_1 + \|\omega\|^2 + \frac{4\nu}{\beta} U_0 \right\}^{-(\nu+d/2)} \\ &\leq E_{U_1} \left\{ \frac{4\nu}{\beta} U_1 + \|\omega\|^2 \right\}^{-(\nu+d/2)} = I(\alpha_1). \end{aligned}$$

□

This lemma indicates that the MLE of the microergodic parameter is monotone when one of its parameters is fixed. This property is used to prove the asymptotics of the MLE for the microergodic parameter. Based on Lemma 1 and Lemma 2, one can be used to show that $\hat{c}_n(\hat{\theta}_n)$ has the same asymptotic properties as $\hat{c}_n(\theta)$ for any fixed θ .

S.3 Technical Proofs

This section contains all the proofs that are not given in the main text.

S.3.1 Proof of Theorem 1

Proof. As $C(0) = \sigma^2 > 0$, it remains to verify the positive definiteness of the function $C(\cdot)$. For any n , all sequences $\{a_i \in \mathbb{R} : i = 1, \dots, n\}$ and all sequences of spatial locations $\{\mathbf{s}_i \in \mathbb{R}^d : i = 1, \dots, n\}$, it follows that

$$\begin{aligned} \sum_{i=1}^n \sum_{j=1}^n a_i a_j C(h_{ij}) &= \sum_{i=1}^n \sum_{j=1}^n a_i a_j \int_0^\infty \mathcal{M}(h_{ij}) \pi(\phi^2) d\phi^2 \\ &= \int_0^\infty \mathbf{a}^\top \mathbf{A} \mathbf{a} \pi(\phi^2) d\phi^2 \geq 0, \end{aligned}$$

where $h_{ij} = \|\mathbf{s}_i - \mathbf{s}_j\|$ and $\mathbf{a} := (a_1, \dots, a_n)^\top$. The matrix $\mathbf{A} := [\mathcal{M}(h_{ij})]_{i,j=1,\dots,n}$ is a covariance matrix constructed via a Matérn covariance function that is positive definite in \mathbb{R}^d for all d , and hence \mathbf{A} is a positive definite matrix, which yields that $\mathbf{a}^\top \mathbf{A} \mathbf{a} \geq 0$. So, the resultant integral is nonnegative, and the function $C(h)$ is positive definite in any Euclidean space.

To derive the form of Equation (3), we start from the gamma mixture representation in Equation (2), and substitute for $\pi(\phi^2)$ the required inverse gamma density.

$$\begin{aligned}
C(h) &= \frac{\sigma^2}{2^\nu \Gamma(\nu)} \int_0^\infty x^{(\nu-1)} \left[\int_0^\infty \phi^{-2\nu} \exp\{-x/(2\phi^2)\} \pi(\phi^2) d\phi^2 \right] \exp(-\nu h^2/x) dx \\
&= \frac{\sigma^2 \beta^\alpha}{2^{\nu+\alpha} \Gamma(\nu) \Gamma(\alpha)} \int_0^\infty x^{(\nu-1)} \left[\int_0^\infty \phi^{-2\nu} \exp\{-x/(2\phi^2)\} \phi^{-2(\alpha+1)} \exp\{-\beta/(2\phi^2)\} d\phi^2 \right] \\
&\quad \times \exp(-\nu h^2/x) dx \\
&= \frac{\sigma^2 \beta^\alpha}{2^{\nu+\alpha} \Gamma(\nu) \Gamma(\alpha)} \int_0^\infty x^{(\nu-1)} \left[\int_0^\infty \phi^{-2(\nu+\alpha+1)} \exp\{-(\beta+x)/(2\phi^2)\} d\phi^2 \right] \\
&\quad \times \exp\{-\nu h^2/x\} dx \\
&= \frac{\sigma^2 \beta^\alpha \Gamma(\nu+\alpha)}{\Gamma(\nu) \Gamma(\alpha)} \int_0^\infty x^{(\nu-1)} (x+\beta)^{-(\nu+\alpha)} \exp(-\nu h^2/x) dx.
\end{aligned}$$

□

S.3.2 Proof of Theorem 2

Proof. (a) Using the property of modified Bessel function (see Abramowitz and Stegun, 1965, p. 375), as $|h| \rightarrow 0$, we can express the Matérn covariance function as

$$\mathcal{M}(h) = \begin{cases} a_1(h) + a_2(\phi, \nu, \sigma^2) |h|^{2\nu} \log |h| + O(|h|^{2\nu}); & \text{when } \nu = 0, 1, 2, \dots, \\ a_3(h) + a_4(\phi, \nu, \sigma^2) |h|^{2\nu} + O(|h|^{2\lceil \nu \rceil}); & \text{otherwise,} \end{cases}$$

where $a_i(h), i = 1, 3$ are of the form $\sum_{k=0}^{\lfloor \nu \rfloor} c_k(\phi, \nu, \sigma^2) h^{2k}$ with $c_k(\phi, \nu, \sigma^2)$ being the coefficients that depend on parameters ϕ, ν, σ^2 . The terms $a_2(\phi, \nu, \sigma^2) = \frac{(-1)^{\nu+1} \sigma^2}{2^{\nu-1} \Gamma(\nu) \Gamma(\nu+1) \phi^{2\nu}}$ and $a_4(\phi, \nu, \sigma^2) = \frac{-\pi \sigma^2}{2^\nu \sin(\nu\pi) \Gamma(\nu) \Gamma(\nu+1) \phi^{2\nu}}$. The terms $a_2(\phi, \nu, \sigma^2) |h|^{2\nu} \log |h|$ and $a_4(\phi, \nu, \sigma^2) |h|^{2\nu}$ are called *principal irregular terms* that determine the differentiability of a random field (see Stein, 1999, p. 32). This implies that the Matérn covariance function is $2m$ times differentiable

if and only if $\nu > m$ for an integer m . By mixing the parameter ϕ^2 over an inverse gamma distribution $\mathcal{IG}(\alpha, \beta/2)$, when $h \rightarrow 0$, the covariance function $C(h)$ can be written as

$$C(h) = \begin{cases} \int_0^\infty a_1(h) \pi(\phi^2) d\phi^2 + \tilde{a}_2(\nu, \sigma^2) |h|^{2\nu} \log |h| + O(|h|^{2\nu}); & \text{when } \nu = 0, 1, 2, \dots, \\ \int_0^\infty a_3(h) \pi(\phi^2) d\phi^2 + \tilde{a}_4(\nu, \sigma^2) |h|^{2\nu} + O(|h|^{2\lceil \nu \rceil}); & \text{otherwise,} \end{cases}$$

where

$$\begin{aligned} \tilde{a}_2(\nu, \sigma^2) &:= \int_0^\infty a_2(\phi, \nu, \sigma^2) \pi(\phi^2) d\phi^2 \\ &= \frac{2(-1)^{\nu+1} \sigma^2}{\Gamma(\nu) \Gamma(\nu+1)} \frac{\Gamma(\nu+\alpha)}{\beta^\nu \Gamma(\alpha)}, \end{aligned}$$

and

$$\begin{aligned} \tilde{a}_4(\nu, \sigma^2) &:= \int_0^\infty a_4(\phi, \nu, \sigma^2) \pi(\phi^2) d\phi^2 \\ &= \frac{-\pi \sigma^2}{\sin(\nu\pi) \Gamma(\nu) \Gamma(\nu+1)} \frac{\Gamma(\nu+\alpha)}{\beta^\nu \Gamma(\alpha)} \\ &= \frac{-\sigma^2 \Gamma(1-\nu)}{\Gamma(\nu+1)} \frac{\Gamma(\nu+\alpha)}{\beta^\nu \Gamma(\alpha)}. \end{aligned}$$

Note that $\tilde{a}_2(\nu, \sigma^2)$ is finite for any positive integer ν and any fixed $\alpha > 0, \beta > 0$, and $\tilde{a}_4(\nu, \sigma^2)$ is finite for $\nu \in (0, \infty) \setminus \mathbb{Z}$ and $\alpha > 0, \beta > 0$. Thus, the covariance $C(h)$ has the same differentiability as the Matérn covariance.

(b) It follows from Theorem 1 that

$$\begin{aligned} C(h) &= \frac{\sigma^2 \beta^\alpha \Gamma(\nu+\alpha)}{\Gamma(\nu) \Gamma(\alpha)} \int_0^\infty \left(\frac{x}{x+\beta} \right)^{\nu+\alpha} x^{-\alpha} \exp(-\nu h^2/x) dx \\ &\stackrel{t=x/2\nu}{=} \frac{\sigma^2 \Gamma(\nu+\alpha)}{(\nu/\beta)^\alpha \Gamma(\nu) \Gamma(\alpha)} \int_0^\infty t^{\nu-1} (t+\beta/(2\nu))^{-(\nu+\alpha)} \exp\{-h^2/(2t)\} dt \\ &= \frac{\sigma^2 \sqrt{2\pi} \Gamma(\nu+\alpha)}{(\nu/\beta)^\alpha \Gamma(\nu) \Gamma(\alpha)} \int_0^\infty \left(\frac{t}{t+\beta/(2\nu)} \right)^{\nu+\alpha} t^{-\alpha-1/2} \frac{1}{\sqrt{2\pi t}} \exp\{-h^2/(2t)\} dt. \end{aligned}$$

Let $L(x) = \left(\frac{x}{x+\beta/(2\nu)} \right)^{\nu+\alpha}$. Then $L(x)$ is a slowly varying function. Viewed as a function of h , the above integral is a Gaussian scale mixture with respect to t . Thus, an application of

Theorem 6.1 of Barndorff-Nielsen et al. (1982) yields

$$\begin{aligned} C(h) &\sim \frac{\sigma^2 \sqrt{2\pi} \Gamma(\nu + \alpha)}{(\nu/\beta)^\alpha \Gamma(\nu) \Gamma(\alpha)} (2\pi)^{-1/2} 2^{\alpha-1} \Gamma(\alpha) |h|^{-2\alpha} L(h^2), \quad \text{as } h \rightarrow \infty, \\ &= \frac{\sigma^2 2^{\alpha-1} \Gamma(\nu + \alpha)}{(\nu/\beta)^\alpha \Gamma(\nu)} |h|^{-2\alpha} L(h^2), \quad \text{as } h \rightarrow \infty. \end{aligned}$$

Thus, the tail decays as $|h|^{-2\alpha} L(h^2)$ when $\alpha > 0$.

□

S.3.3 Proof of Proposition 1

Proof. The proof consists of two parts. We first show that the CH covariance $C(h)$ belongs to the family of the continuous functions, Φ_d , from $[0, \infty)$ to \mathbb{R} . Then we use Theorem 6.1 of Barndorff-Nielsen et al. (1982) to derive the tail behavior of the spectral density.

The family Φ_d is nested with $\Phi_1 \supset \Phi_2 \supset \cdots \supset \Phi_\infty$ with $\Phi_\infty := \bigcap_{d \geq 1} \Phi_d$ being the family of radial functions that are positive definite on any d -dimensional Euclidean space. Schoenberg (1938) shows that any member ϕ that is in the family Φ_d can be written as a scale mixture with any probability measure F :

$$\phi(h) = \int_0^\infty h^{-(d-2)/2} \mathcal{J}_{(d-2)/2}(\omega h) dF(\omega), \quad h \geq 0,$$

where $\mathcal{J}_\nu(\cdot)$ is the ordinary Bessel function (see 9.1.20 of Abramowitz and Stegun, 1965). It is well-known that the Matérn covariance is a member of Φ_∞ for any positive values of ϕ and ν . The CH covariance class as a scale mixture of the Matérn class is also a member of Φ_∞ . The Fourier transform of $f \in \Phi_d$, denoted by $\mathcal{F}(f)$, is available in a convenient form (Yaglom, 1987) with

$$\mathcal{F}(f)(\omega) = (2\pi)^{-d/2} \int_0^\infty (u\omega)^{-(d-2)/2} \mathcal{J}_{(d-2)/2}(u\omega) u^{d-1} f(u) du, \quad \omega \geq 0.$$

Notice that the Matérn covariance function (1) has spectral density

$$\begin{aligned} f_{\mathcal{M}}(\omega) &= (2\pi)^{-d/2} \int_0^\infty (\omega h)^{-(d-2)/2} \mathcal{J}_{(d-2)/2}(\omega h) h^{d-1} \mathcal{M}(h) dh, \\ &= \frac{\sigma^2 (\sqrt{2\nu}/\phi)^{2\nu}}{\pi^{d/2} ((\sqrt{2\nu}/\phi)^2 + \omega^2)^{\nu+d/2}}. \end{aligned}$$

Thus, the spectral density of the covariance function $C(h)$ is

$$\begin{aligned}
f(\omega) &= (2\pi)^{-d/2} \int_0^\infty (\omega h)^{-(d-2)/2} \mathcal{J}_{(d-2)/2}(\omega h) h^{d-1} \int_0^\infty \mathcal{M}(h) \pi(\phi^2) d\phi^2 dh \\
&= \frac{\sigma^2 2^{\nu-\alpha} \nu^\nu (\beta/2)^\alpha}{\Gamma(\alpha)} \int_0^\infty \frac{\phi^{-2\nu}}{\pi^{d/2} (2\nu\phi^{-2} + \omega^2)^{\nu+d/2}} \phi^{-2(\alpha+1)} \exp\{-\beta/(2\phi^2)\} d\phi^2 \\
&= \frac{\sigma^2 2^{\nu-\alpha} \nu^\nu \beta^\alpha}{\pi^{d/2} \Gamma(\alpha)} \int_0^\infty (2\nu\phi^{-2} + \omega^2)^{-\nu-d/2} \phi^{-2(\nu+\alpha+1)} \exp\{-\beta/(2\phi^2)\} d\phi^2.
\end{aligned}$$

where the above spectral density is finite for $\alpha > d/2$ and is infinite for $\alpha \in (0, d/2]$. When $\alpha \in (0, d/2]$, the Fourier transform needs to be computed in the Schwartz space of test functions such that the spectral density could still be defined. Here we are only interested in deriving the tail behavior of the spectral density.

To derive the tail behavior, we make the change of variable $\phi^2 = \beta t / \omega^2$. The spectral density above can be expressed as

$$\begin{aligned}
f(\omega) &= \frac{\sigma^2 2^{\nu-\alpha} \nu^\nu \beta^\alpha}{\pi^{d/2} \Gamma(\alpha)} \omega^{2\alpha-d} \int_0^\infty ((2\nu/\beta)t^{-1} + 1)^{-(\nu+d/2)} t^{-(\nu+\alpha+1)} \exp\{-\omega^2/(2t)\} dt \\
&= \frac{\sigma^2 2^{\nu-\alpha} \nu^\nu}{\pi^{d/2} \beta^\nu \Gamma(\alpha)} (2\pi)^{1/2} \omega^{2\alpha-d} \int_0^\infty \left(\frac{t}{2\nu/\beta + t} \right)^{(\nu+d/2)} t^{(-\nu-\alpha+1/2)-1} \frac{1}{\sqrt{2\pi t}} \\
&\quad \times \exp\{-\omega^2/(2t)\} dt.
\end{aligned}$$

Let $L(x) = \left\{ \frac{x}{x+\beta/(2\nu)} \right\}^{\nu+d/2}$. Then $L(x)$ is a slowly varying function at ∞ . The above integral is also a Gaussian scale mixture. Thus, an application of Theorem 6.1 of Barndorff-Nielsen et al. (1982) yields that as $|\omega| \rightarrow \infty$,

$$\begin{aligned}
f(\omega) &\sim \frac{\sigma^2 2^{\nu-\alpha} \nu^\nu}{\pi^{d/2} \beta^\nu \Gamma(\alpha)} (2\pi)^{1/2} \omega^{2\alpha-d} (2\pi)^{-1/2} 2^{1/2+(\nu+\alpha-1/2)} |\omega|^{-2(\nu+\alpha-1/2)-1} L(\omega^2) \\
&= \frac{\sigma^2 2^{2\nu} \nu^\nu \Gamma(\nu+\alpha)}{\pi^{d/2} \beta^\nu \Gamma(\alpha)} \omega^{-(2\nu+d)} L(\omega^2).
\end{aligned}$$

□

S.3.4 Proof of Theorem 3

Proof. Let $f_i(\omega), i = 1, 2$ be the spectral densities with parameters $\{\sigma_i^2, \beta_i, \alpha_i, \nu\}$ for two covariance functions $C_1(\cdot), C_2(\cdot)$. The condition (S.1) says the spectral density $f_i(\omega)$ is bounded at zero and ∞ when $\omega \rightarrow \infty$. In fact, let $\lambda = 2\nu + d$. Then, one can show that

$$\lim_{\omega \rightarrow \infty} f_1(\omega) |\omega|^{2\nu+d} = \frac{\sigma_1^2 \beta_1^{-\nu} 2^{2\nu} \nu^\nu \Gamma(\nu + \alpha_1)}{\pi^{d/2} \Gamma(\alpha_1)}.$$

Thus, the condition (S.1) is satisfied.

We first show the sufficiency. Assume that the condition in Equation (5) holds. To prove the equivalence of two measures, it suffices to show that the condition (S.2) is satisfied. Notice that as $\omega \rightarrow \infty$,

$$\begin{aligned} \left| \frac{f_1(\omega) - f_2(\omega)}{f_1(\omega)} \right| &= \left| \frac{\{\omega^2 + \beta_2/(2\nu)\}^{-(\nu+d/2)}}{\{\omega^2 + \beta_1/(2\nu)\}^{-(\nu+d/2)}} - 1 \right| \\ &\leq \omega^{-(2\nu+d)} \left| \{\omega^2 + \beta_2/(2\nu)\}^{\nu+d/2} - \{\omega^2 + \beta_1/(2\nu)\}^{\nu+d/2} \right| \\ &\leq \left| \{1 + (\beta_2/2\nu)\omega^{-2}\}^{\nu+d/2} - \{1 + (\beta_1/2\nu)\omega^{-2}\}^{\nu+d/2} \right| \\ &\leq \left| \{1 + (\nu + d/2)(\beta_2/2\nu)\omega^{-2} + O(\omega^{-4})\} \right. \\ &\quad \left. - \{1 + (\nu + d/2)(\beta_1/2\nu)\omega^{-2} + O(\omega^{-4})\} \right| \\ &\leq |\beta_1 - \beta_2|(\nu + d/2)/(2\nu)\omega^{-2} + O(\omega^{-4}). \end{aligned}$$

The integral in (S.2) is finite for $d = 1, 2, 3$. Therefore, the two measures are equivalent.

It remains to show the necessary condition. Suppose

$$\frac{\sigma_1^2 \beta_1^{-\nu} \Gamma(\nu + \alpha_1)}{\Gamma(\alpha_1)} \neq \frac{\sigma_2^2 \beta_2^{-\nu} \Gamma(\nu + \alpha_2)}{\Gamma(\alpha_2)}.$$

Let,

$$\sigma_0^2 = \sigma_2^2 \frac{\beta_2^{-\nu} \Gamma(\alpha_1) \Gamma(\nu + \alpha_2)}{\beta_1^{-\nu} \Gamma(\alpha_2) \Gamma(\nu + \alpha_1)}.$$

Then,

$$\frac{\sigma_0^2 \beta_1^{-\nu} \Gamma(\nu + \alpha_1)}{\Gamma(\alpha_1)} = \frac{\sigma_2^2 \beta_2^{-\nu} \Gamma(\nu + \alpha_2)}{\Gamma(\alpha_2)},$$

and the two covariograms $C(h; \nu, \alpha_1, \beta_1, \sigma_0^2)$ and $C(h; \nu, \alpha_1, \beta_1, \sigma_1^2)$ define two equivalent measures. It remains to show that $C(h; \nu, \alpha_1, \beta_1, \sigma_0^2)$ and $C(h; \nu, \alpha_2, \beta_2, \sigma_2^2)$ defines two equivalence Gaussian measures. The rest of arguments follow from the poof in Theorem 2 of Zhang (2004). \square

S.3.5 Proof of Theorem 4

Proof. Let $k_1 = \sigma_1^2 \frac{2^{2\nu} \nu^\nu \Gamma(\nu + \alpha)}{\pi^{d/2} \beta^\nu \Gamma(\alpha)}$ and $k_2 = \sigma_2^2 (2\nu)^\nu \phi^{-2\nu} / \pi^{d/2}$. Then the condition in Equation (6) implies that $k_1 = k_2$. It follows that as $|\omega| \rightarrow \infty$,

$$\begin{aligned} \left| \frac{f_1(\omega) - f_2(\omega)}{f_1(\omega)} \right| &= \left| \frac{k_2}{k_1} (\omega^2 + 2\nu/\phi^2)^{-(\nu+d/2)} (\omega^2 + \beta/(2\nu))^{(\nu+d/2)} - 1 \right| \\ &= (\omega^2 + 2\nu/\phi^2)^{-(\nu+d/2)} \times \left| k_2/k_1 (\omega^2 + 2\nu/\phi^2)^{\nu+d/2} \right. \\ &\quad \left. - (\omega^2 + \beta/(2\nu))^{\nu+d/2} \right| \\ &\leq \omega^{-(2\nu+d)} \times \left| (\omega^2 + 2\nu/\phi^2)^{\nu+d/2} - (\omega^2 + \beta/(2\nu))^{\nu+d/2} \right| \\ &\leq \left| \{1 + (2\nu/\phi^2)\omega^{-2}\}^{-(\nu+d/2)} - \{1 + \beta/(2\nu)\omega^{-2}\}^{(\nu+d/2)} \right| \\ &\leq \left| \{1 + (2\nu/\phi^2)(\nu + d/2)\omega^{-2} + O(\omega^{-4})\} - \{1 + \beta/(2\nu)(\nu + d/2)\omega^{-2} \right. \\ &\quad \left. + O(\omega^{-4})\} \right|. \\ &\leq |2\nu/\phi^2 - \beta/(2\nu)|(\nu + d/2)\omega^{-2} + O(\omega^{-4}). \end{aligned}$$

The integral in (S.2) is finite for $d = 1, 2, 3$. Therefore, these two measures are equivalent. \square

S.3.6 Proof of Theorem 5

Proof. We define sequences, $\hat{c}_n(\alpha, \beta_L)$, $\hat{c}_n(\alpha, \beta_U)$, $\hat{c}_n(\alpha_L, \beta)$, and $\hat{c}_n(\alpha_U, \beta)$. It follows from Lemma 2 that $\hat{c}_n(\alpha, \beta_L) \leq \hat{c}_n(\alpha, \hat{\beta}_n) \leq \hat{c}_n(\alpha, \hat{\beta}_U)$ and $\hat{c}_n(\alpha_U, \beta) \leq \hat{c}_n(\hat{\alpha}_n, \beta) \leq \hat{c}_n(\alpha_U, \beta)$. Applying Theorem 1 yields the desired results for $\hat{c}_n(\alpha, \hat{\beta}_n)$ and $\hat{c}_n(\hat{\alpha}_n, \beta)$. To show the result for $\hat{c}_n(\hat{\theta}_n) = \hat{c}_n(\hat{\alpha}_n, \hat{\beta}_n)$, it suffices to show that $\hat{c}_n(\alpha_U, \beta_L) \leq \hat{c}_n(\hat{\alpha}_n, \hat{\beta}_n) \leq \hat{c}_n(\alpha_L, \beta_U)$ according to Lemma 2. In fact, we have, $\hat{c}_n(\alpha_U, \beta_L) \leq \hat{c}_n(\alpha_U, \hat{\beta}) \leq \hat{c}_n(\hat{\alpha}_n, \hat{\beta}_n)$ and $\hat{c}_n(\hat{\alpha}_n, \hat{\beta}_n) \leq \hat{c}_n(\alpha_L, \hat{\beta}_n) \leq \hat{c}_n(\alpha_L, \beta_U)$. \square

S.3.7 Proof of Theorem 6

Proof. Part (a) and Part (b) can be proven by applying Theorem 1 and Theorem 2 of Stein (1993).

Let $f_i(\omega)$ be the spectral density of the CH class $C(h; \nu, \alpha_i, \beta_i, \sigma_i^2)$ with $i = 1, 2$. Note that $\lim_{\omega \rightarrow \infty} f_i(\omega)|\omega|^{2\nu+d}$ is finite. If the condition in Equation (5) is satisfied, then,

$$\lim_{\omega \rightarrow \infty} \frac{f_2(\omega)}{f_1(\omega)} = \lim_{\omega \rightarrow \infty} \frac{f_2(\omega)|\omega|^{2\nu+d}}{f_1(\omega)|\omega|^{2\nu+d}} = 1.$$

The proof of Part (c) is analogous to the proof of Theorem 4 in Kaufman and Shaby (2013). Let

$$\sigma_1^2 := \sigma_0^2(\beta_1/\beta_0)^\nu \frac{\Gamma(\nu + \alpha_0)\Gamma(\alpha_1)}{\Gamma(\nu + \alpha_1)\Gamma(\alpha_0)}.$$

Then \mathcal{P}_0 and \mathcal{P}_1 define two equivalence measures. We write

$$\frac{\text{Var}_{\nu, \theta_1, \hat{\sigma}_n^2} \{\hat{Z}_n(\theta_1) - Z(\mathbf{s}_0)\}}{\text{Var}_{\nu, \theta_0, \sigma_0^2} \{\hat{Z}_n(\theta_1) - Z(\mathbf{s}_0)\}} = \frac{\text{Var}_{\nu, \theta_1, \hat{\sigma}_n^2} \{\hat{Z}_n(\theta_1) - Z(\mathbf{s}_0)\}}{\text{Var}_{\nu, \theta_1, \sigma_1^2} \{\hat{Z}_n(\theta_1) - Z(\mathbf{s}_0)\}} \frac{\text{Var}_{\nu, \theta_1, \sigma_1^2} \{\hat{Z}_n(\theta_1) - Z(\mathbf{s}_0)\}}{\text{Var}_{\nu, \theta_0, \sigma_0^2} \{\hat{Z}_n(\theta_1) - Z(\mathbf{s}_0)\}}.$$

According to Part (b) of Theorem 6, it suffices to show that almost surely

$$\frac{\text{Var}_{\nu, \theta_1, \hat{\sigma}_n^2} \{\hat{Z}_n(\theta_1) - Z(\mathbf{s}_0)\}}{\text{Var}_{\nu, \theta_1, \sigma_1^2} \{\hat{Z}_n(\theta_1) - Z(\mathbf{s}_0)\}} \rightarrow 1.$$

By Equation (9),

$$\frac{\text{Var}_{\nu, \theta_1, \hat{\sigma}_n^2} \{\hat{Z}_n(\theta_1) - Z(\mathbf{s}_0)\}}{\text{Var}_{\nu, \theta_1, \sigma_1^2} \{\hat{Z}_n(\theta_1) - Z(\mathbf{s}_0)\}} = \frac{\hat{\sigma}_n^2}{\sigma_1^2}.$$

Note that under \mathcal{P}_1 , we have $\hat{\sigma}_n^2 \sim (\sigma_0^2/n)\chi_n$, and hence $\hat{\sigma}_n^2$ converges almost surely to σ_0^2 as $n \rightarrow \infty$. As \mathcal{P}_0 is equivalent to \mathcal{P}_1 , It follows from Theorem 1 that $\hat{\sigma}_n^2 \rightarrow \sigma_1^2$, almost surely. \square

S.3.8 Proof of Theorem 7

Proof. Let $f_0(\omega)$ be the spectral density of the Matérn covariance function $\mathcal{M}(h; \nu, \phi, \sigma_0^2)$ and $f_1(\omega)$ be the spectral density of the covariance function $C(h; \nu, \alpha, \beta, \sigma_1^2)$. Notice that the spectral density of the Matérn covariance satisfies the condition (S.1). It suffices to show that $\lim_{\omega \rightarrow \infty} f_1(\omega)/f_0(\omega) =$

1. Let $k_0 = \sigma_0^2 \phi^{-2\nu}$ and $k_1 = \sigma_1^2 (\beta/2)^{-\nu} \Gamma(\nu + \alpha) / \Gamma(\alpha)$. If $k_0 = k_1$, it follows that

$$\lim_{\omega \rightarrow \infty} \frac{f_1(\omega)}{f_0(\omega)} = \lim_{\omega \rightarrow \infty} \frac{f_1(\omega) |\omega|^{2\nu+d}}{f_0(\omega) |\omega|^{2\nu+d}} = \lim_{\omega \rightarrow \infty} \frac{k_1}{k_0} (2\nu \phi^{-2} \omega^{-2} + 1)^{\nu+d/2} = k_1/k_0 = 1.$$

Thus, the covariance function $C(h; \nu, \alpha, \beta, \sigma_1^2)$ yields an asymptotically equivalent BLP as the Matérn covariance $\mathcal{M}(h; \nu, \phi, \sigma_0^2)$. □

S.4 Examples to Illustrate Asymptotic Normality

As shown in Section 3.2, each individual parameter in the CH model cannot be estimated consistently, however, the microergodic parameter can be estimated consistently.

To study the finite sample performance of the asymptotic properties of MLE for the microergodic parameter, we simulate 1000 realizations from a zero-mean Gaussian process with the CH class over 100-by-100 regular grid in the unit domain $\mathcal{D} = [0, 1] \times [0, 1]$. As there are no clear guidelines to pick the sample sizes such that the finite sample performances can appropriately reflect the asymptotic results, we randomly select $n = 4000, 5000, 6000$ locations from these 10,000 grid points. The variance parameter is fixed at 1 for all realizations. We consider two different values for the smoothness parameter ν at 0.5 and 1.5, three different values for the tail decay parameter α at 0.5, 2 and 5. The scale parameter β is chosen such that the effective range is 0.6 or 0.9. Although all the theoretical results in Section 3 are valid for $\alpha > d/2$, we also run the simulation setting with $\alpha = 0.5$ to see whether there is any interesting numerical results compared to cases where $\alpha > d/2$.

Let $C(h; \nu, \alpha_0, \beta_0, \sigma_0^2)$ be the true covariance. We use $\hat{c}_n(\theta)$ to denote the maximum likelihood estimator of the microergodic parameter $c(\theta_0) = \sigma_0^2 \beta_0^{-\nu} \Gamma(\nu + \alpha_0) / \Gamma(\alpha_0)$ for any θ . Then the 95% confidence interval for $c(\theta_0)$ is given by $\hat{c}_n(\theta) \pm 1.96 \sqrt{2\hat{c}_n(\theta)^2/n}$. Lemma 1 and Theorem 5 show that this interval is asymptotically valid when n is large and $\alpha > d/2$ for (1) arbitrarily fixed θ , (2) $\theta = (\alpha, \hat{\beta}_n)$, (3) $\theta = (\hat{\alpha}_n, \beta)$ and (4) $\theta = (\hat{\alpha}_n, \hat{\beta}_n)$. In this simulation study, we primarily focus on the finite sample performance of $\hat{c}_n(\theta)$, where $\theta = (\alpha_0, 0.5\beta_0)$, $\theta = (\alpha_0, \beta_0)$, $\theta = (\alpha_0, 2\beta_0)$, $\theta = (\alpha_0, \hat{\beta}_n)$, and $\theta = (\hat{\alpha}_n, \hat{\beta}_n)$. Exhaustive simulations with all other settings of θ is considered future work. Let

$$\zeta := \frac{\sqrt{n}\{\hat{c}_n(\theta) - c(\theta_0)\}}{\sqrt{2}c(\theta_0)}.$$

Then ζ should asymptotically follow the standard normal distribution. Based on these 1000 realizations, we compute the empirical coverage probability of the 95% percentile confidence interval, bias and root-mean-square error (RMSE) for $c(\theta_0)$ and compare the quantiles of ζ with the standard normal quantiles.

The results are reported in Table S.1, Table S.2 and Table S.3 of the Supplementary Material. They can be summarized as follows. When the true parameters are used, i.e., $\theta = \theta_0$, as expected, the sampling distribution of $\hat{c}_n(\theta_0)$ gives the best normal approximation and converges to the asymptotic distribution in Lemma 1 when n increases. The sampling distribution of $\hat{c}_n(\theta)$ can be highly biased and approach to the truth can be very slow with increase in n . Fixing β at a larger value gives better empirical results than fixing β at a small value. When the scale parameter is chosen to be its maximum likelihood estimator, i.e., $\beta = \hat{\beta}_n$, the sampling distribution of $\hat{c}_n(\alpha, \hat{\beta}_n)$ converges to the asymptotic distribution given in Theorem 5 as n increases. When α is small, e.g., $\alpha = 0.5$, the sampling distributions of $\hat{c}_n(\theta)$, with $(\alpha_0, 0.5\beta_0)$, $(\alpha_0, 2\beta_0)$, $(\alpha_0, \hat{\beta}_n)$ and $(\hat{\alpha}_n, \hat{\beta}_n)$ substituted for θ , has noticeable biases. As the tail decay parameter or the effective range increases, the sampling distributions of $\hat{c}_n(\theta)$ have smaller biases. As ν becomes smaller, the sampling distributions of $\hat{c}_n(\theta)$ approaches the truth better with increase in n . When $\nu = 0.5$ and $\alpha \in \{2, 5\}$, these sampling distributions have negligible biases as n increases. When both α and β are substituted by their maximum likelihood estimator, the sampling distribution of $\hat{c}_n(\theta)$ has smaller bias and gives better approximation to the true asymptotic distribution given in Theorem 5 as n increases for $\alpha > d/2 = 1$.

When α is fixed at its true value and β is estimated by maximum likelihood method, the MLE of the microergodic parameter, $\hat{c}_n(\alpha, \hat{\beta}_n)$, gives better finite sample performance than the cases where β is misspecified. When both α and β are estimated by maximum likelihood method, the MLE of the microergodic parameter, $\hat{c}_n(\hat{\alpha}_n, \hat{\beta}_n)$, also gives better finite sample performance than the cases where β is misspecified and α is fixed at its true value. One would also expect that this is true when either α or β is misspecified at incorrect values. In general, the MLE of the microergodic parameter has better finite sampler performance than those with any individual parameter fixed at an incorrect value in the microergodic parameter. Theorem 5 requires $\alpha > d/2$ in order to derive asymptotic results for $\hat{c}_n(\hat{\alpha}_n, \hat{\beta}_n)$. However, it is interesting to observe from these simulation results that $\hat{c}_n(\theta)$ seems to converge to a normal distribution even when $\alpha < d/2$, i.e., when $\alpha = 0.5$. It is an open problem to determine the exact distribution that the maximum likelihood estimator $\hat{c}_n(\hat{\alpha}_n, \hat{\beta}_n)$ of the microergodic parameter converges to asymptotically when α and β are substituted with their maximum likelihood estimators for true $\alpha_0 \in (0, d/2]$.

Table S.1. Percentiles of ζ and CVG, bias, and RMSE of $\hat{c}_n(\theta)$ when $\alpha_0 = 0.5$.

Settings		5%	25%	50%	75%	95%	CVG	bias	RMSE
$\mathcal{N}(0, 1)$		-1.6449	-0.6749	0	0.6749	1.6449	0.95	0	
$ER = 0.6, \nu = 0.5$									
θ									
$\alpha = \alpha_0, \beta = \beta_0$	$n = 4000$	-1.449	-0.542	0.009	0.686	1.767	0.955	0.020	0.327
	$n = 5000$	-1.469	-0.665	-0.077	0.696	1.573	0.965	-0.003	0.289
	$n = 6000$	-1.705	-0.618	0.056	0.662	1.847	0.929	0.010	0.280
$\alpha = \alpha_0, \beta = 0.5\beta_0$	$n = 4000$	2.113	3.098	3.730	4.424	5.549	0.044	1.259	1.308
	$n = 5000$	2.129	2.930	3.578	4.439	5.347	0.040	1.097	1.140
	$n = 6000$	1.798	3.015	3.705	4.397	5.606	0.071	1.005	1.049
$\alpha = \alpha_0, \beta = 2\beta_0$	$n = 4000$	-3.471	-2.608	-2.073	-1.420	-0.394	0.415	-0.676	0.746
	$n = 5000$	-3.480	-2.693	-2.114	-1.395	-0.519	0.404	-0.611	0.676
	$n = 6000$	-3.688	-2.623	-1.967	-1.376	-0.214	0.462	-0.543	0.606
$\alpha = \alpha_0, \beta = \hat{\beta}_n$	$n = 4000$	-1.871	-0.711	0.095	1.000	2.244	0.889	0.047	0.428
	$n = 5000$	-1.912	-0.767	0.022	0.881	2.134	0.881	0.013	0.371
	$n = 6000$	-2.016	-0.760	0.096	0.862	2.097	0.879	0.019	0.343
$\alpha = \hat{\alpha}_n, \beta = \hat{\beta}_n$	$n = 4000$	-1.778	-0.875	0.000	0.925	2.382	0.887	0.030	0.446
	$n = 5000$	-2.129	-0.816	0.026	0.893	2.227	0.870	0.019	0.395
	$n = 6000$	-2.268	-0.911	-0.015	0.865	2.117	0.875	-0.006	0.363
$ER = 0.6, \nu = 1.5$									
θ									
$\alpha = \alpha_0, \beta = \beta_0$	$n = 4000$	-1.654	-0.604	-0.014	0.701	1.776	0.949	12.650	370.7
	$n = 5000$	-1.430	-0.687	-0.046	0.672	1.576	0.969	0.283	312.0
	$n = 6000$	-1.731	-0.649	0.070	0.710	1.740	0.929	7.182	307.5
$\alpha = \alpha_0, \beta = 0.5\beta_0$	$n = 4000$	26.20	27.77	28.82	30.03	31.76	0.000	10495	10513
	$n = 5000$	27.09	28.35	29.37	30.55	31.99	0.000	9567	9581
	$n = 6000$	27.22	28.79	29.85	30.89	32.68	0.000	8860	8874
$\alpha = \alpha_0, \beta = 2\beta_0$	$n = 4000$	-13.70	-12.93	-12.48	-11.99	-11.21	0.000	-4526	4534
	$n = 5000$	-13.99	-13.35	-12.90	-12.36	-11.62	0.000	-4177	4184
	$n = 6000$	-14.47	-13.61	-13.11	-12.58	-11.80	0.000	-3886	3893
$\alpha = \alpha_0, \beta = \hat{\beta}_n$	$n = 4000$	-2.993	-1.121	0.172	1.515	3.505	0.670	72.52	732.5
	$n = 5000$	-2.823	-1.155	0.146	1.452	3.398	0.700	49.49	624.8
	$n = 6000$	-3.068	-1.090	0.235	1.433	3.093	0.733	44.59	543.1
$\alpha = \hat{\alpha}_n, \beta = \hat{\beta}_n$	$n = 4000$	-3.887	-1.656	0.061	1.681	4.142	0.565	9.059	895.5
	$n = 5000$	-3.607	-1.643	0.055	1.497	4.142	0.592	16.27	772.1
	$n = 6000$	-4.107	-1.678	-0.206	1.488	3.774	0.592	-70.59	832.3
$ER = 0.9, \nu = 0.5$									
θ									
$\alpha = \alpha_0, \beta = \beta_0$	$n = 4000$	-1.589	-0.557	-0.013	0.669	1.748	0.955	0.007	0.220
	$n = 5000$	-1.429	-0.654	0.065	0.759	1.683	0.978	0.012	0.190
	$n = 6000$	-1.512	-0.591	0.004	0.702	1.768	0.943	0.009	0.179
$\alpha = \alpha_0, \beta = 0.5\beta_0$	$n = 4000$	0.628	1.679	2.278	2.967	4.052	0.399	0.513	0.563
	$n = 5000$	0.727	1.546	2.306	2.994	3.958	0.420	0.454	0.496
	$n = 6000$	0.548	1.543	2.200	2.888	4.013	0.445	0.403	0.444
$\alpha = \alpha_0, \beta = 2\beta_0$	$n = 4000$	-2.812	-1.808	-1.259	-0.595	0.440	0.769	-0.272	0.346
	$n = 5000$	-2.620	-1.846	-1.170	-0.478	0.379	0.760	-0.229	0.295
	$n = 6000$	-2.635	-1.756	-1.187	-0.477	0.586	0.799	-0.205	0.270
$\alpha = \alpha_0, \beta = \hat{\beta}_n$	$n = 4000$	-1.856	-0.688	0.087	0.911	1.946	0.905	0.021	0.262
	$n = 5000$	-1.587	-0.696	0.062	0.822	1.930	0.926	0.018	0.220
	$n = 6000$	-1.646	-0.589	0.045	0.833	2.008	0.918	0.020	0.202
$\alpha = \hat{\alpha}_n, \beta = \hat{\beta}_n$	$n = 4000$	-1.876	-0.748	0.082	0.882	2.157	0.887	0.016	0.276
	$n = 5000$	-1.865	-0.692	0.023	0.853	1.994	0.902	0.014	0.233
	$n = 6000$	-1.884	-0.744	0.006	0.901	1.978	0.904	0.008	0.213
$ER = 0.9, \nu = 1.5$									
θ									
$\alpha = \alpha_0, \beta = \beta_0$	$n = 4000$	-1.598	-0.618	-0.015	0.663	1.747	0.958	2.284	106.8
	$n = 5000$	-1.426	-0.647	0.063	0.774	1.711	0.977	6.598	92.45
	$n = 6000$	-1.660	-0.623	0.059	0.685	1.743	0.945	2.287	87.41
$\alpha = \alpha_0, \beta = 0.5\beta_0$	$n = 4000$	17.15	18.51	19.42	20.44	21.94	0.000	2096	2102
	$n = 5000$	17.34	18.50	19.50	20.42	21.83	0.000	1877	1881
	$n = 6000$	17.06	18.45	19.36	20.24	21.70	0.000	1699	1703
$\alpha = \alpha_0, \beta = 2\beta_0$	$n = 4000$	-10.02	-9.207	-8.722	-8.151	-7.284	0.000	-934.2	938.3
	$n = 5000$	-9.964	-9.263	-8.691	-8.092	-7.331	0.000	-8.835	839.5
	$n = 6000$	-10.13	-9.280	-8.717	-8.159	-7.26	0.000	-766.2	769.8
$\alpha = \alpha_0, \beta = \hat{\beta}_n$	$n = 4000$	-2.455	-0.993	0.029	1.282	2.953	0.771	15.62	180.4
	$n = 5000$	-2.224	-1.038	-0.031	1.140	2.706	0.789	8.661	151.8
	$n = 6000$	-2.259	-0.918	0.082	1.152	2.586	0.803	11.20	131.2
$\alpha = \hat{\alpha}_n, \beta = \hat{\beta}_n$	$n = 4000$	-3.178	-1.316	-0.002	1.215	3.289	0.691	1.887	208.8
	$n = 5000$	-3.055	-1.211	-0.003	1.229	3.129	0.708	2.440	178.3
	$n = 6000$	-2.820	-1.285	0.006	1.236	3.051	0.710	0.875	156.7

Table S.2. Percentiles of ζ and CVG, bias, and RMSE of $\hat{c}_n(\theta)$ when $\alpha_0 = 2$.

Settings		5%	25%	50%	75%	95%	CVG	bias	RMSE
$\mathcal{N}(0, 1)$		-1.6449	-0.6749	0	0.6749	1.6449	0.95	0	
$ER = 0.6, v = 0.5$									
θ									
$\alpha = \alpha_0, \beta = \beta_0$	$n = 4000$	-1.557	-0.604	-0.013	0.691	1.759	0.954	0.004	0.099
	$n = 5000$	-1.442	-0.614	0.003	0.723	1.575	0.962	0.002	0.086
	$n = 6000$	-1.689	-0.462	0.093	0.728	1.970	0.947	0.003	0.084
$\alpha = \alpha_0, \beta = 0.5\beta_0$	$n = 4000$	-1.072	-0.128	0.486	1.179	2.264	0.921	0.052	0.113
	$n = 5000$	-0.999	-0.179	0.493	1.183	2.047	0.939	0.043	0.097
	$n = 6000$	-1.315	-0.010	0.556	1.184	2.396	0.929	0.041	0.094
$\alpha = \alpha_0, \beta = 2\beta_0$	$n = 4000$	-1.801	-0.860	-0.258	0.440	1.505	0.949	-0.021	0.101
	$n = 5000$	-1.680	-0.840	-0.232	0.479	1.347	0.946	-0.018	0.088
	$n = 6000$	-1.880	-0.681	-0.136	0.517	1.756	0.931	-0.012	0.084
$\alpha = \alpha_0, \beta = \hat{\beta}_n$	$n = 4000$	-1.616	-0.600	0.040	0.758	1.796	0.954	0.008	0.103
	$n = 5000$	-1.443	-0.583	0.070	0.752	1.705	0.962	0.006	0.088
	$n = 6000$	-1.564	-0.505	0.171	0.774	1.941	0.938	0.008	0.087
$\alpha = \hat{\alpha}_n, \beta = \hat{\beta}_n$	$n = 4000$	-1.576	-0.546	0.140	0.798	1.880	0.944	0.014	0.104
	$n = 5000$	-1.426	-0.565	0.094	0.785	1.747	0.956	0.009	0.089
	$n = 6000$	-1.595	-0.614	0.079	0.764	1.882	0.953	0.007	0.085
$ER = 0.6, v = 1.5$									
θ									
$\alpha = \alpha_0, \beta = \beta_0$	$n = 4000$	-1.567	-0.624	-0.010	0.689	1.764	0.952	0.103	2.513
	$n = 5000$	-1.469	-0.633	0.005	0.734	1.620	0.958	0.083	2.200
	$n = 6000$	-1.729	-0.614	0.016	0.592	1.646	0.953	-0.013	2.027
$\alpha = \alpha_0, \beta = 0.5\beta_0$	$n = 4000$	1.226	2.227	2.885	3.622	4.748	0.215	7.351	7.840
	$n = 5000$	1.056	2.005	2.772	3.469	4.427	0.257	6.145	6.586
	$n = 6000$	0.725	1.861	2.602	3.180	4.350	0.296	5.225	5.657
$\alpha = \alpha_0, \beta = 2\beta_0$	$n = 4000$	-2.801	-1.876	-1.283	-0.593	0.433	0.749	-3.103	3.948
	$n = 5000$	-2.590	-1.829	-1.185	-0.497	0.385	0.765	-2.612	3.379
	$n = 6000$	-2.807	-1.771	-1.128	-0.565	0.493	0.779	-2.350	3.073
$\alpha = \alpha_0, \beta = \hat{\beta}_n$	$n = 4000$	-1.613	-0.649	0.093	0.790	1.923	0.928	0.223	2.701
	$n = 5000$	-1.417	-0.648	0.046	0.818	1.821	0.957	0.197	2.332
	$n = 6000$	-1.623	-0.655	0.056	0.691	1.793	0.954	0.071	2.111
$\alpha = \hat{\alpha}_n, \beta = \hat{\beta}_n$	$n = 4000$	-1.558	-0.598	0.095	0.811	1.977	0.921	0.301	2.759
	$n = 5000$	-1.543	-0.594	0.040	0.798	1.827	0.950	0.186	2.342
	$n = 6000$	-1.604	-0.569	0.090	0.763	1.827	0.946	0.198	2.132
$ER = 0.9, v = 0.5$									
θ									
$\alpha = \alpha_0, \beta = \beta_0$	$n = 4000$	-1.574	-0.594	-0.026	0.666	1.776	0.952	0.002	0.066
	$n = 5000$	-1.458	-0.664	-0.052	0.638	1.547	0.962	-0.001	0.057
	$n = 6000$	-1.742	-0.548	0.145	0.809	1.784	0.942	0.005	0.055
$\alpha = \alpha_0, \beta = 0.5\beta_0$	$n = 4000$	-1.319	-0.321	0.254	0.930	2.042	0.938	0.020	0.069
	$n = 5000$	-1.220	-0.411	0.185	0.904	1.817	0.962	0.014	0.059
	$n = 6000$	-1.567	-0.366	0.385	1.022	2.052	0.925	0.017	0.058
$\alpha = \alpha_0, \beta = 2\beta_0$	$n = 4000$	-1.704	-0.723	-0.158	0.524	1.635	0.950	-0.007	0.066
	$n = 5000$	-1.579	-0.786	-0.173	0.517	1.424	0.963	-0.007	0.057
	$n = 6000$	-1.862	-0.653	0.024	0.700	1.646	0.950	-0.001	0.054
$\alpha = \alpha_0, \beta = \hat{\beta}_n$	$n = 4000$	-1.586	-0.578	0.022	0.695	1.799	0.948	0.005	0.068
	$n = 5000$	-1.440	-0.615	-0.006	0.696	1.648	0.959	0.001	0.058
	$n = 6000$	-1.653	-0.450	0.244	0.880	1.646	0.930	0.009	0.055
$\alpha = \hat{\alpha}_n, \beta = \hat{\beta}_n$	$n = 4000$	-1.572	-0.550	0.123	0.789	1.862	0.950	0.008	0.068
	$n = 5000$	-1.378	-0.541	0.097	0.798	1.782	0.957	0.007	0.059
	$n = 6000$	-1.659	-0.595	0.055	0.727	1.786	0.954	0.003	0.055
$ER = 0.9, v = 1.5$									
θ									
$\alpha = \alpha_0, \beta = \beta_0$	$n = 4000$	-1.589	-0.595	-0.015	0.700	1.748	0.955	0.028	0.744
	$n = 5000$	-1.454	-0.668	-0.029	0.673	1.531	0.966	-0.006	0.638
	$n = 6000$	-1.701	-0.671	-0.098	0.572	1.747	0.940	-0.031	0.652
$\alpha = \alpha_0, \beta = 0.5\beta_0$	$n = 4000$	-0.026	0.961	1.579	2.307	3.369	0.675	1.205	1.434
	$n = 5000$	-0.117	0.805	1.443	2.165	3.003	3.705	0.978	1.183
	$n = 6000$	-0.371	0.705	1.327	1.957	3.189	0.764	0.813	1.037
$\alpha = \alpha_0, \beta = 2\beta_0$	$n = 4000$	-2.288	-1.288	-0.722	-0.002	1.009	0.886	-0.498	0.886
	$n = 5000$	-2.098	-1.348	-0.706	-0.010	0.858	0.916	-0.447	0.771
	$n = 6000$	-2.312	-1.309	-0.728	-0.050	1.071	0.887	-0.411	0.742
$\alpha = \alpha_0, \beta = \hat{\beta}_n$	$n = 4000$	-1.684	-0.599	0.092	0.751	1.805	0.934	0.058	0.780
	$n = 5000$	-1.468	-0.698	-0.003	0.696	1.641	0.966	0.007	0.658
	$n = 6000$	-1.670	-0.725	-0.068	0.660	1.775	0.931	-0.023	0.644
$\alpha = \hat{\alpha}_n, \beta = \hat{\beta}_n$	$n = 4000$	-1.532	-0.611	0.100	0.820	1.903	0.934	0.080	0.781
	$n = 5000$	-1.422	-0.584	0.050	0.746	1.745	0.959	0.049	0.664
	$n = 6000$	-1.498	-0.544	0.068	0.810	1.843	0.950	0.042	0.618

Table S.3. Percentiles of ζ and CVG, bias, and RMSE of $\hat{c}_n(\theta)$ when $\alpha_0 = 5$.

Settings		5%	25%	50%	75%	95%	CVG	bias	RMSE
$\mathcal{N}(0, 1)$		-1.6449	-0.6749	0	0.6749	1.6449	0.95	0	
$ER = 0.6, \nu = 0.5$									
θ									
$\alpha = \alpha_0, \beta = \beta_0$	$n = 4000$	-1.612	-0.659	-0.049	0.655	1.661	0.954	0.000	0.085
	$n = 5000$	-1.468	-0.636	-0.027	0.685	1.683	0.961	0.002	0.074
	$n = 6000$	-1.633	-0.560	0.079	0.723	1.751	0.940	0.003	0.070
$\alpha = \alpha_0, \beta = 0.5\beta_0$	$n = 4000$	-1.273	-0.289	0.319	1.010	2.038	0.942	0.030	0.091
	$n = 5000$	-1.183	-0.311	0.298	1.033	2.054	0.942	0.027	0.079
	$n = 6000$	-1.261	-0.245	0.401	1.023	2.070	0.932	0.025	0.074
$\alpha = \alpha_0, \beta = 2\beta_0$	$n = 4000$	-1.757	-0.829	-0.222	0.479	1.477	0.945	-0.015	0.086
	$n = 5000$	-1.616	-0.793	-0.191	-0.500	-1.520	0.958	-0.011	0.074
	$n = 6000$	-1.787	-0.709	-0.071	0.556	1.587	0.936	-0.007	0.070
$\alpha = \alpha_0, \beta = \hat{\beta}_n$	$n = 4000$	-1.607	-0.633	0.000	0.690	1.705	0.951	0.003	0.087
	$n = 5000$	-1.434	-0.591	0.030	0.719	1.766	0.953	0.005	0.075
	$n = 6000$	-1.609	-0.564	0.094	0.758	1.822	0.930	0.006	0.071
$\alpha = \hat{\alpha}_n, \beta = \hat{\beta}_n$	$n = 4000$	-1.556	-0.538	0.142	0.813	1.884	0.948	0.012	0.089
	$n = 5000$	-1.378	-0.514	0.116	0.835	1.762	0.958	0.010	0.076
	$n = 6000$	-1.530	-0.557	0.100	0.758	1.832	0.950	0.008	0.070
$ER = 0.6, \nu = 1.5$									
θ									
$\alpha = \alpha_0, \beta = \beta_0$	$n = 4000$	-1.611	-0.651	-0.015	0.676	1.748	0.957	0.026	1.179
	$n = 5000$	-1.409	-0.606	0.052	0.727	1.705	0.958	0.069	1.031
	$n = 6000$	-1.346	-0.495	0.146	0.763	1.660	0.950	0.114	0.930
$\alpha = \alpha_0, \beta = 0.5\beta_0$	$n = 4000$	0.153	1.146	1.783	2.469	3.601	0.618	2.132	2.463
	$n = 5000$	0.109	1.070	1.720	2.432	3.475	0.628	1.818	2.113
	$n = 6000$	0.053	1.018	1.675	2.311	3.351	0.653	1.623	1.886
$\alpha = \alpha_0, \beta = 2\beta_0$	$n = 4000$	-2.308	-1.383	-0.802	-0.088	0.934	0.875	-0.877	1.456
	$n = 5000$	-2.093	-1.323	-0.675	0.004	0.964	0.909	-0.685	1.224
	$n = 6000$	-1.985	-1.186	-0.521	0.083	0.993	0.929	-0.538	1.059
$\alpha = \alpha_0, \beta = \hat{\beta}_n$	$n = 4000$	-1.664	-0.641	0.069	0.757	1.802	0.951	0.070	1.239
	$n = 5000$	-1.362	-0.615	0.080	0.792	1.788	0.956	0.105	1.074
	$n = 6000$	-1.368	-0.588	0.177	0.809	1.812	0.950	0.129	0.966
$\alpha = \hat{\alpha}_n, \beta = \hat{\beta}_n$	$n = 4000$	-1.528	-0.569	0.138	0.845	1.937	0.929	0.181	1.263
	$n = 5000$	-1.342	-0.522	0.105	0.838	1.822	0.956	0.150	1.065
	$n = 6000$	-1.468	-0.518	0.102	0.842	1.920	0.937	0.142	1.003
$ER = 0.9, \nu = 0.5$									
θ									
$\alpha = \alpha_0, \beta = \beta_0$	$n = 4000$	-1.567	-0.602	-0.013	0.681	1.759	0.955	0.002	0.057
	$n = 5000$	-1.482	-0.664	-0.034	0.643	1.563	0.961	0.000	0.049
	$n = 6000$	-1.513	-0.615	0.077	0.637	1.745	0.953	0.002	0.045
$\alpha = \alpha_0, \beta = 0.5\beta_0$	$n = 4000$	-1.377	-0.423	0.179	0.871	1.956	0.947	0.013	0.058
	$n = 5000$	-1.333	-0.478	0.153	0.835	1.743	0.961	0.009	0.050
	$n = 6000$	-1.357	-0.468	0.233	0.800	1.894	0.947	0.009	0.046
$\alpha = \alpha_0, \beta = 2\beta_0$	$n = 4000$	-1.663	-0.708	-0.109	0.587	1.646	0.957	-0.004	0.057
	$n = 5000$	-1.554	-0.765	-0.121	0.556	1.465	0.958	-0.005	0.049
	$n = 6000$	-1.605	-0.692	-0.006	0.559	1.655	0.942	-0.002	0.045
$\alpha = \alpha_0, \beta = \hat{\beta}_n$	$n = 4000$	-1.571	-0.593	0.016	0.716	1.744	0.951	0.004	0.058
	$n = 5000$	-1.424	-0.653	-0.007	0.669	1.638	0.962	0.001	0.049
	$n = 6000$	-1.462	-0.572	0.095	0.704	1.803	0.949	0.003	0.045
$\alpha = \hat{\alpha}_n, \beta = \hat{\beta}_n$	$n = 4000$	-1.574	-0.539	0.106	0.803	1.853	0.952	0.007	0.059
	$n = 5000$	-1.327	-0.537	0.134	0.810	1.778	0.960	0.007	0.049
	$n = 6000$	-1.606	-0.601	0.058	0.713	1.756	0.956	0.003	0.046
$ER = 0.9, \nu = 1.5$									
θ									
$\alpha = \alpha_0, \beta = \beta_0$	$n = 4000$	-1.574	-0.616	-0.015	0.661	1.764	0.955	0.009	0.345
	$n = 5000$	-1.414	-0.617	0.015	0.741	1.612	0.974	0.017	0.298
	$n = 6000$	-1.743	-0.591	0.066	0.677	1.795	0.933	0.008	0.292
$\alpha = \alpha_0, \beta = 0.5\beta_0$	$n = 4000$	-0.614	0.325	0.969	1.631	2.762	0.837	0.351	0.498
	$n = 5000$	-0.587	0.274	0.936	1.652	2.593	0.857	0.299	0.428
	$n = 6000$	-0.978	0.198	0.889	1.566	2.643	0.870	0.248	0.389
$\alpha = \alpha_0, \beta = 2\beta_0$	$n = 4000$	-1.988	-1.042	-0.448	0.234	1.285	0.933	-0.139	0.369
	$n = 5000$	-1.784	-1.013	-0.373	0.330	1.207	0.956	-0.105	0.313
	$n = 6000$	-2.094	-0.968	-0.301	0.312	1.420	0.925	-0.097	0.306
$\alpha = \alpha_0, \beta = \hat{\beta}_n$	$n = 4000$	-1.590	-0.609	0.029	0.720	1.791	0.943	0.021	0.356
	$n = 5000$	-1.364	-0.605	0.055	0.779	1.677	0.967	0.025	0.303
	$n = 6000$	-1.648	-0.608	0.107	0.709	1.823	0.947	0.015	0.296
$\alpha = \hat{\alpha}_n, \beta = \hat{\beta}_n$	$n = 4000$	-1.533	-0.549	0.113	0.849	1.836	0.940	0.047	0.369
	$n = 5000$	-1.387	-0.526	0.111	0.798	1.733	0.961	0.039	0.307
	$n = 6000$	-1.352	-0.534	0.111	0.765	1.755	0.956	0.039	0.281

S.5 Additional Simulation Examples

S.5.1 Predictive Performance with Different Sample Sizes

In this section, we use the same simulation settings as in Section 4 but with $n = 500$ and 1000 observations for parameter estimation. The simulation setup here is the same as the one considered in Section 4. For $n = 500$ observations, the results are shown in Figure S.2 for Case 1, Figure S.3 for Case 2, and Figure S.4 for Case 3. For $n = 1000$ observations, the results are shown in Figure S.5 for Case 1, Figure S.6 for Case 2, and Figure S.7 for Case 3. To conclude, the CH class is very flexible since it can allow different smoothness behaviors in the same way as the Matérn class and can allow different degrees of tail behaviors that can capture the one in the GC class.

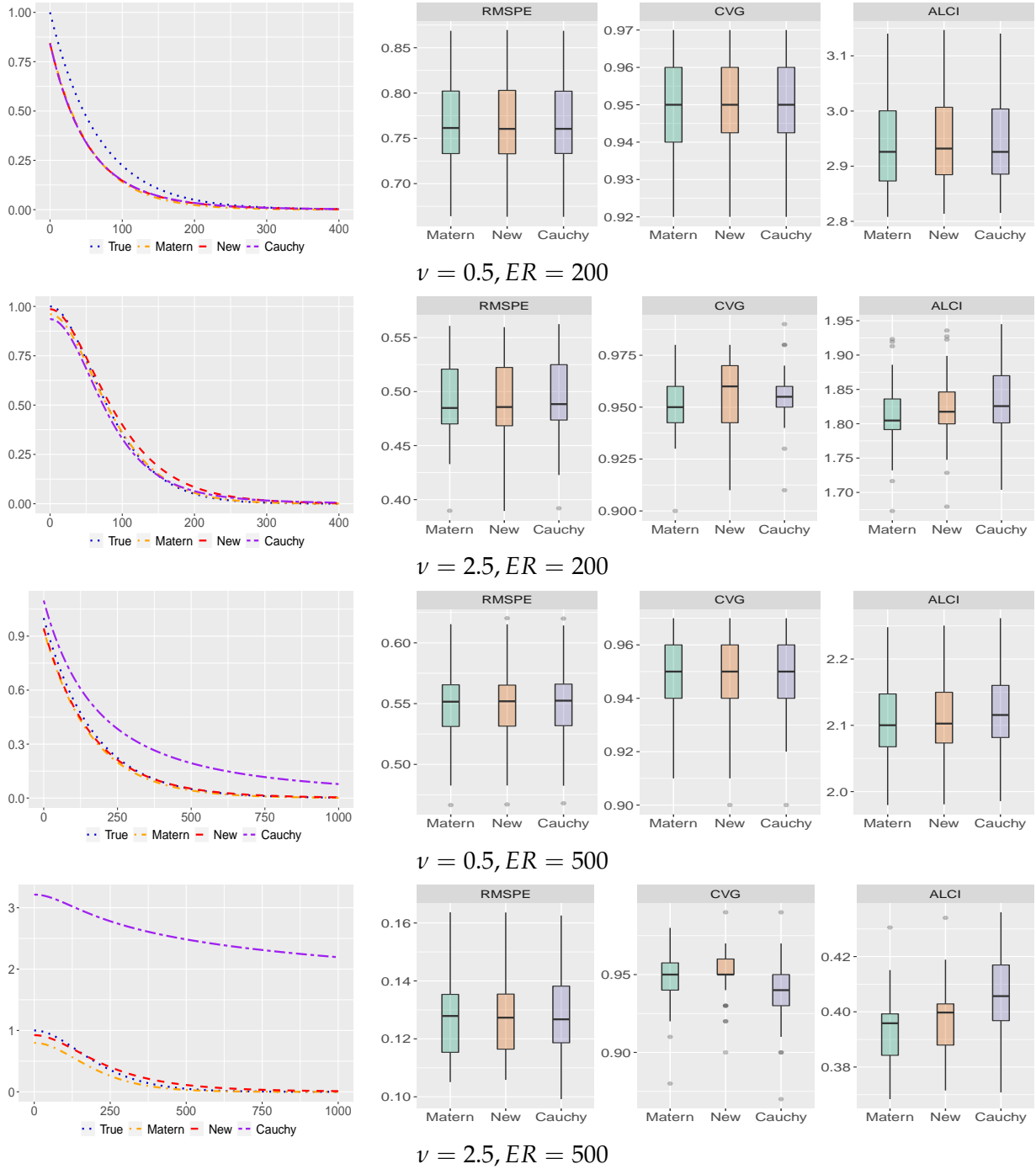


Fig. S.2. Case 1: Comparison of predictive performance and estimated covariance structures when the true covariance is the Matérn class with 500 observations. The predictive performance is evaluated at 10-by-10 regular grids in the square domain. These figures summarize the predictive measures based on RMSPE, CVG and ALCI under 30 simulated realizations.

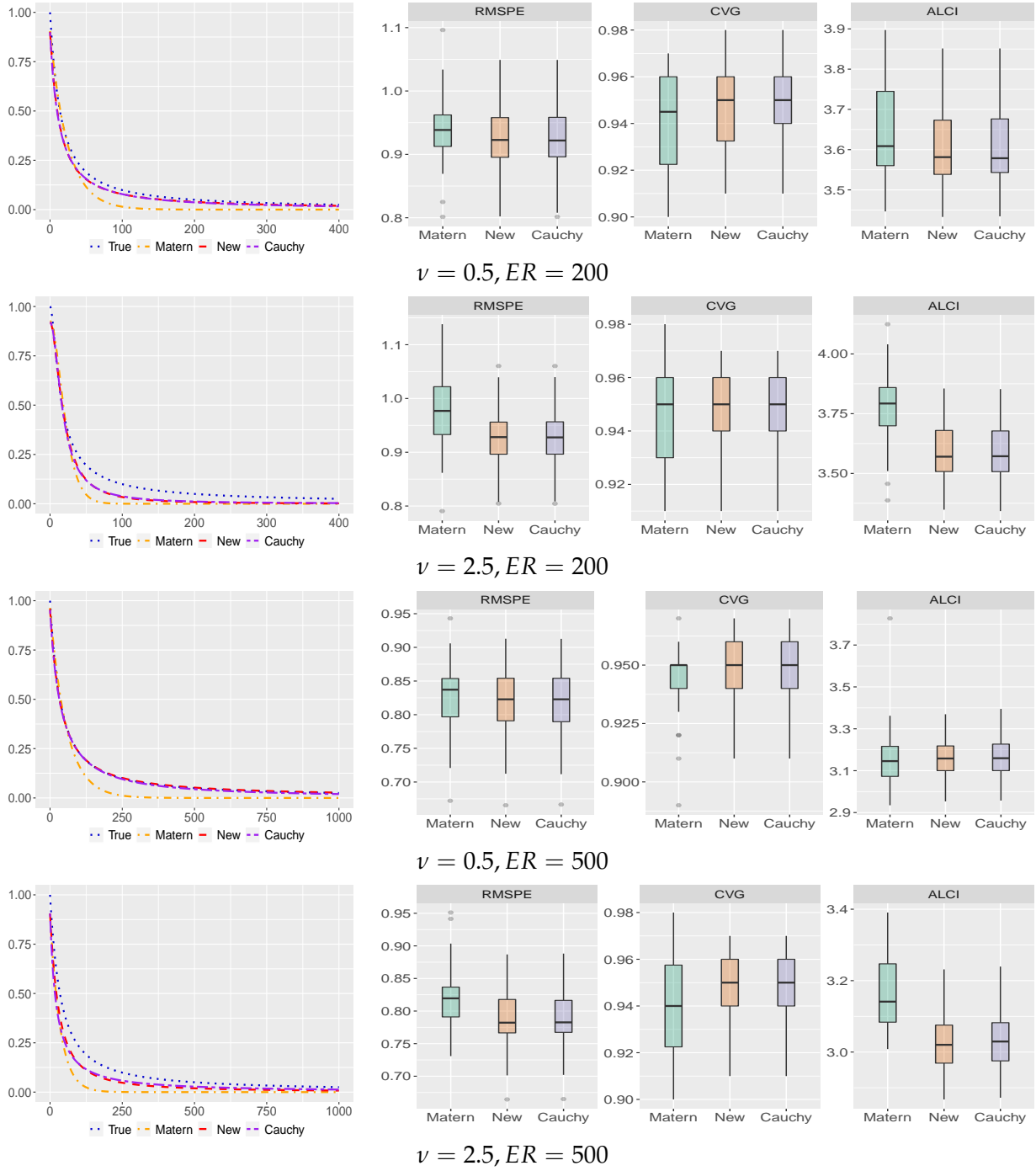


Fig. S.3. Case 2: Comparison of predictive performance and estimated covariance structures when the true covariance is the CH class with 500 observations. The predictive performance is evaluated at 10-by-10 regular grids in the square domain. These figures summarize the predictive measures based on RMSPE, CVG and ALCI under 30 simulated realizations.

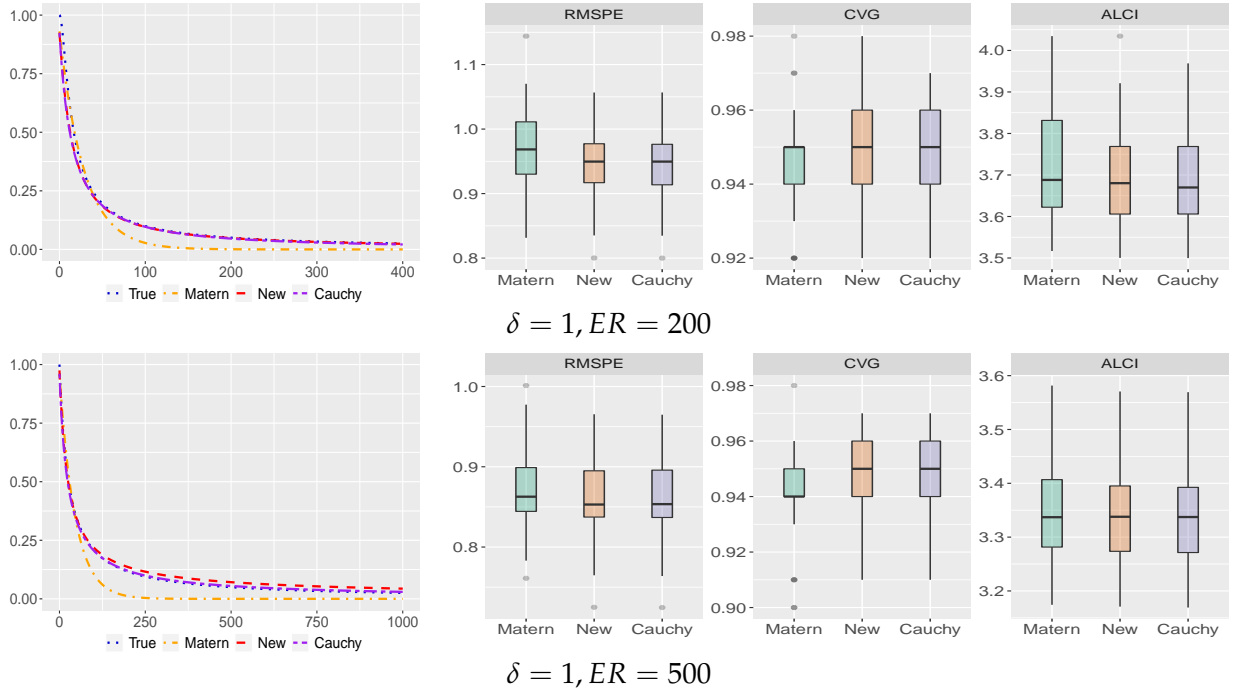


Fig. S.4. Case 3: Comparison of predictive performance and estimated covariance structures when the true covariance is the GC class with 500 observations. The predictive performance is evaluated at 10-by-10 regular grids in the square domain. These figures summarize the predictive measures based on RMSPE, CVG and ALCI under 30 simulated realizations.

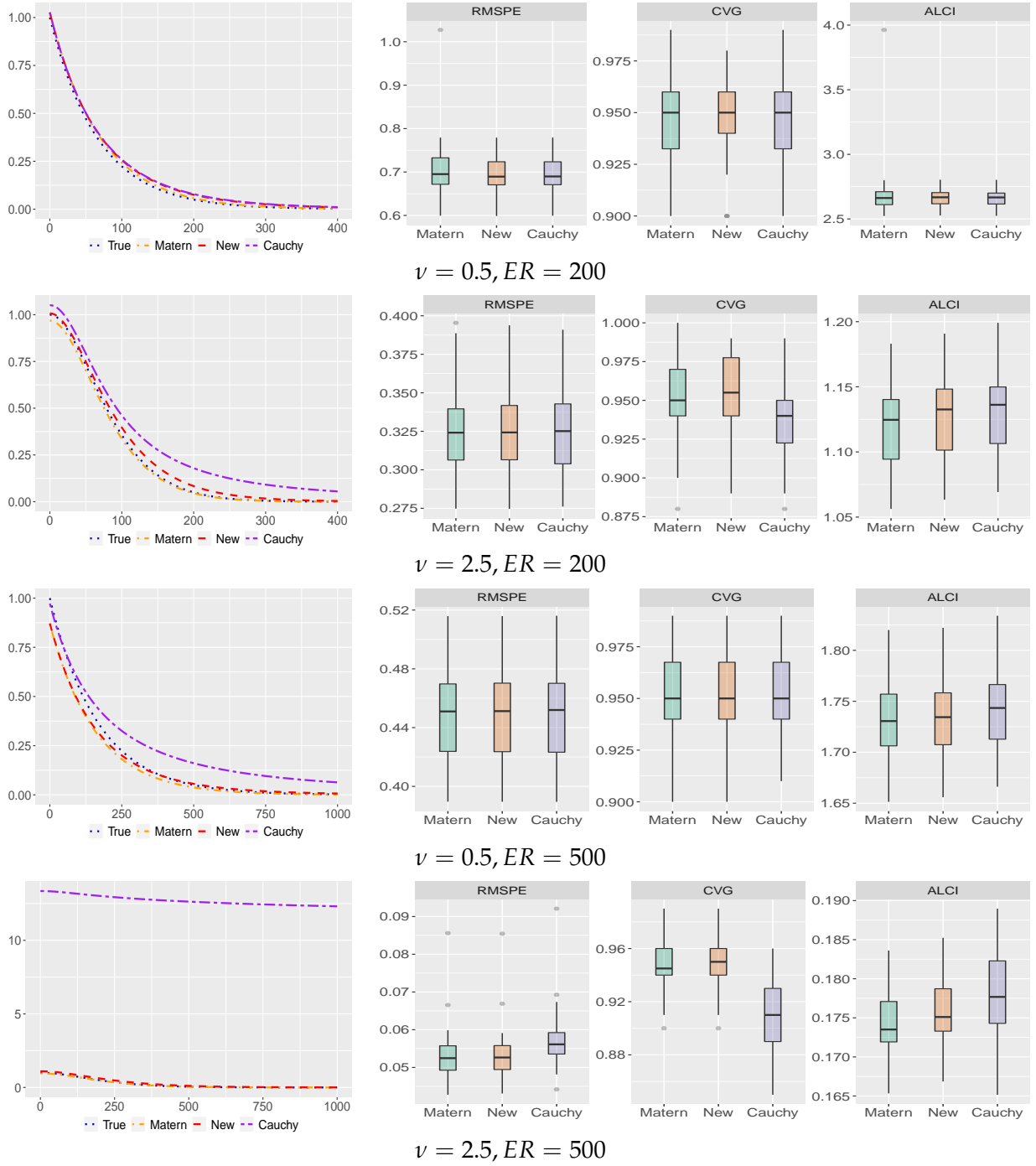


Fig. S.5. Case 1: Comparison of predictive performance and estimated covariance structures when the true covariance is the Matérn class with 1000 observations. The predictive performance is evaluated at 10-by-10 regular grids in the square domain. These figures summarize the predictive measures based on RMSPE, CVG and ALCI under 30 simulated realizations.

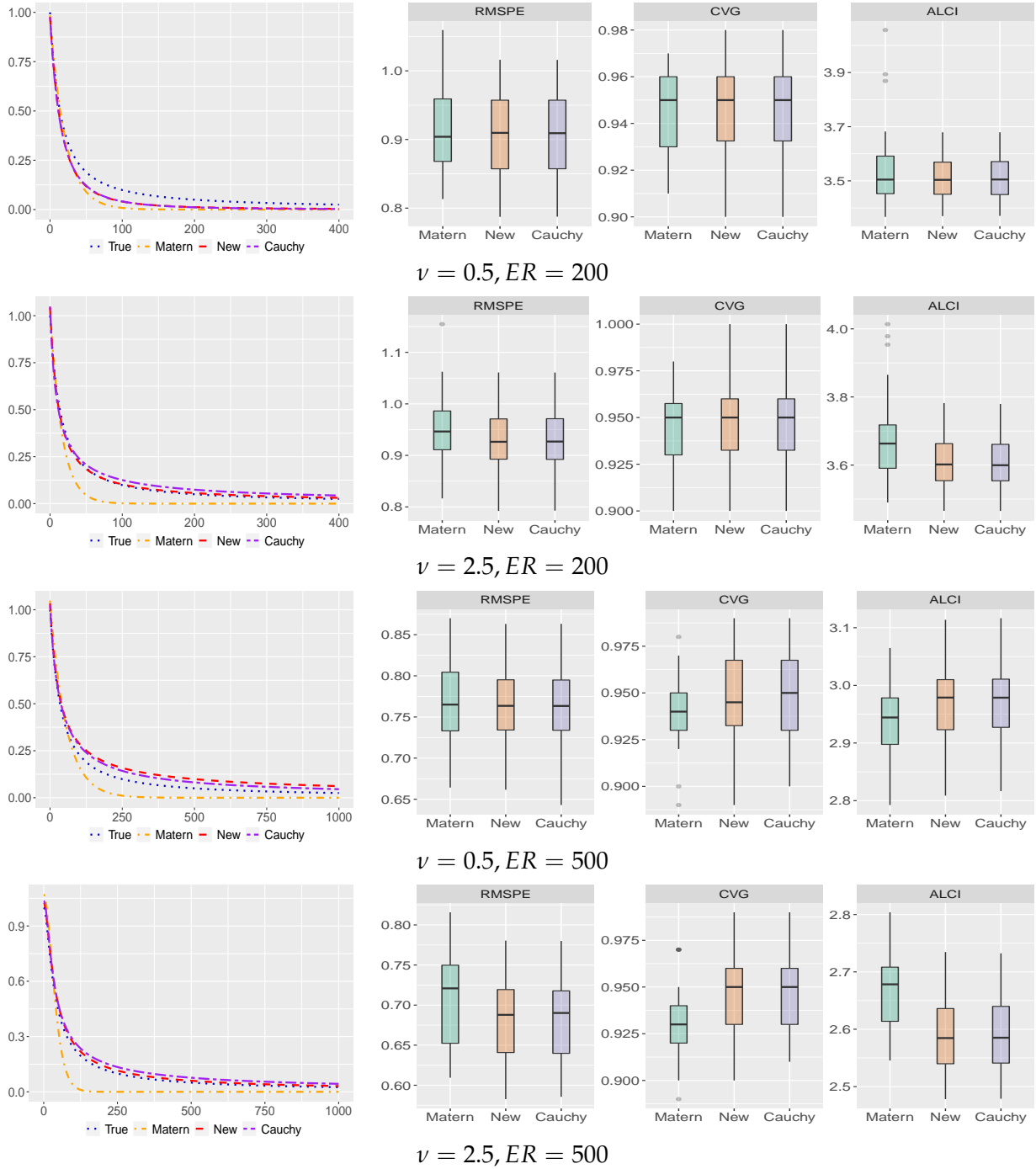


Fig. S.6. Case 2: Comparison of predictive performance and estimated covariance structures when the true covariance is the CH class with 1000 observations. The predictive performance is evaluated at 10-by-10 regular grids in the square domain. These figures summarize the predictive measures based on RMSPE, CVG and ALCI under 30 simulated realizations.

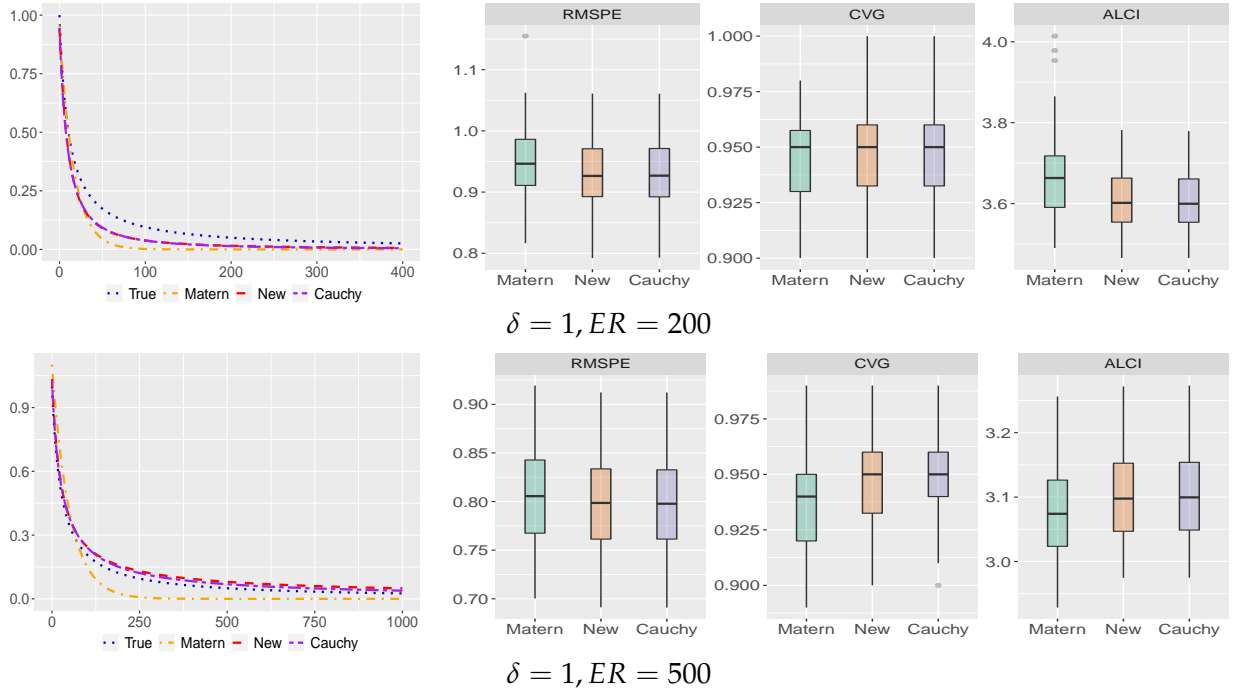


Fig. S.7. Case 3: Comparison of predictive performance and estimated covariance structures when the true covariance is the GC class with 1000 observations. The predictive performance is evaluated at 10-by-10 regular grids in the square domain. These figures summarize the predictive measures based on RMSPE, CVG and ALCI under 30 simulated realizations.

S.5.2 Simulation with a Tensor Product of Covariance Functions

In this section, we study the predictive performance of the CH class with a product form, i.e., $r(\|\mathbf{s} - \mathbf{u}\|) = \prod_{i=1}^d R(|s_i - u_i|; \boldsymbol{\theta}_i)$, where $R(\cdot; \boldsymbol{\theta}_i)$ is an isotropic covariance function with parameter $\boldsymbol{\theta}_i$. This product form of covariance functions allows different properties along different coordinate directions (or input space) and has been widely used in uncertainty quantification and machine learning.

We simulate the true processes under the Matérn class and the CH class with effective range fixed at 200 and 500. For the smoothness parameter, we consider $\nu = 0.5, 2.5$. The tail decay parameter in the CH class is chosen to be 0.5. As each dimension has a different range parameter or scale parameter, we choose these parameters in each dimension such that their correlation will be $0.5^{1/2}$ at distance 200 and 500. This will guarantee the overall effective range will be 200 and 500, respectively. For each simulation setting, the true process is simulated at $n = 100, 500, 1000$ locations. The GC class has a smoothness parameter that is specified as in Section 4. The prediction locations are the same as those in Section 4.

In the first case where the true process has a product of Matérn covariance functions, the prediction results under the Matérn class, the CH class and the GC class are shown in panels from (a) to (f) of Figure S.8. As expected, the Matérn class and the CH class yield indistinguishable predictive performance in terms of RMSPE, CVG, and ALCI. However, the GC class has much worse performance than the other two covariance classes. In the second case where the true process has a product of CH functions, the prediction results under these three covariance classes are shown in panels from (g) to (l) of Figure S.8. As expected, the CH class yields much better prediction results than the Matérn class, since the Matérn class has an exponentially decaying tail that is not able to capture the tail behavior in the CH class. It is worth noting that the GC class yields much worse predictive performance than the other two covariance classes. This is quite different from the situation when the true process does not have a product covariance form.

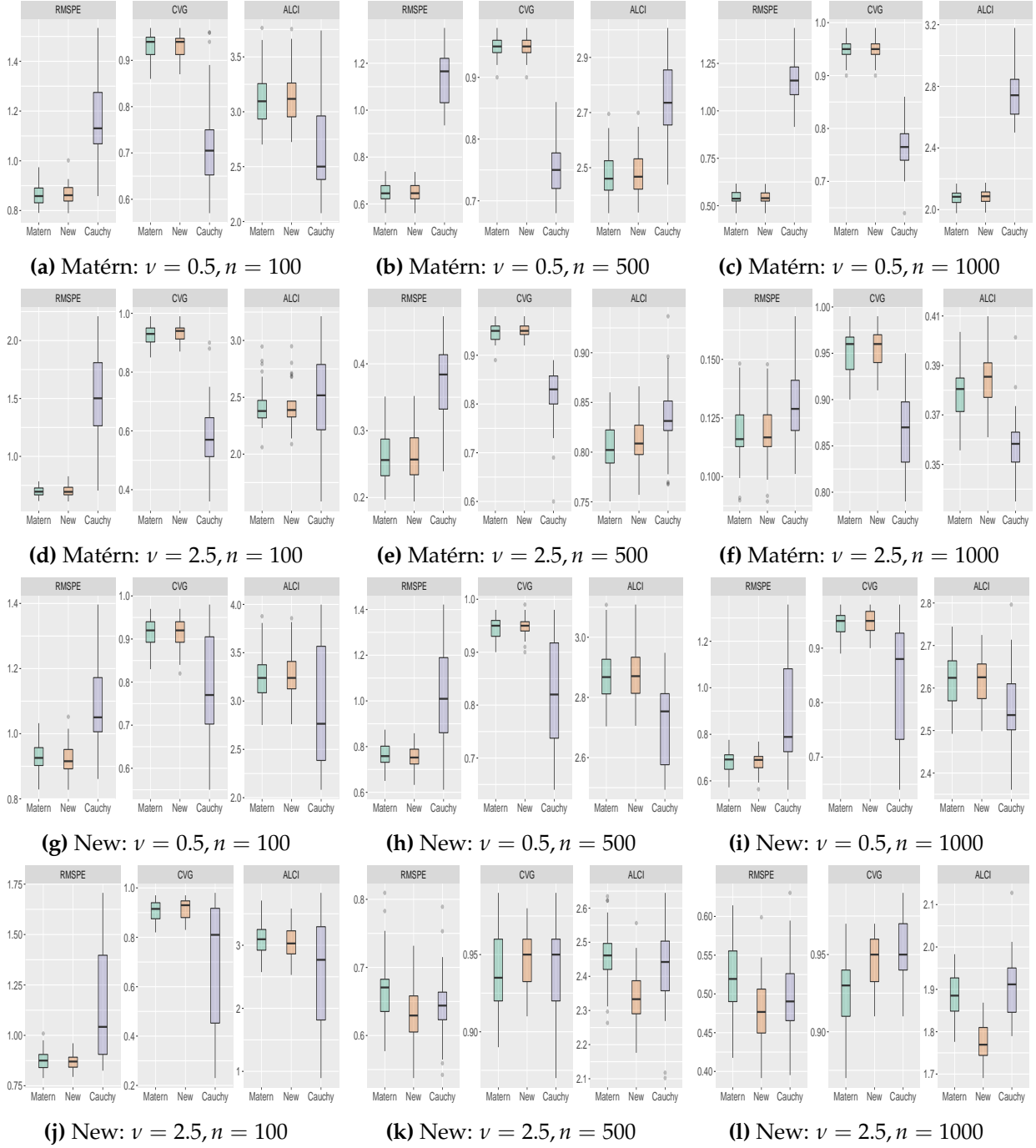


Fig. S.8. Predictive performance over 10-by-10 regular grids under three covariance classes when the true process has a product form of covariance structures. The predictive performance is studied under different smoothness parameters, effective ranges and number of observation locations.

S.6 Additional Numerical Results

This section contains parameter estimation results and figures referenced in Section 5. Table S.4 shows the estimated parameters under the Matérn covariance model and the CH covariance in the cross-validation study of Section 5. Figure S.9 compares kriging predictors and associated standard errors under the CH class and Matérn class in the cross-validation study of Section 5.

Table S.4. Cross-validation results based on the Matérn covariance model and the CH covariance model.

	Matérn class		CH class	
	$\nu = 0.5$	$\nu = 1.5$	$\nu = 0.5$	$\nu = 1.5$
b	411.1	411.1	411.0	411.0
σ^2	1.679	1.439	1.750	1.585
ϕ	160.5	104.1	—	—
α	—	—	0.381	0.353
β	—	—	6426.7	3439.9

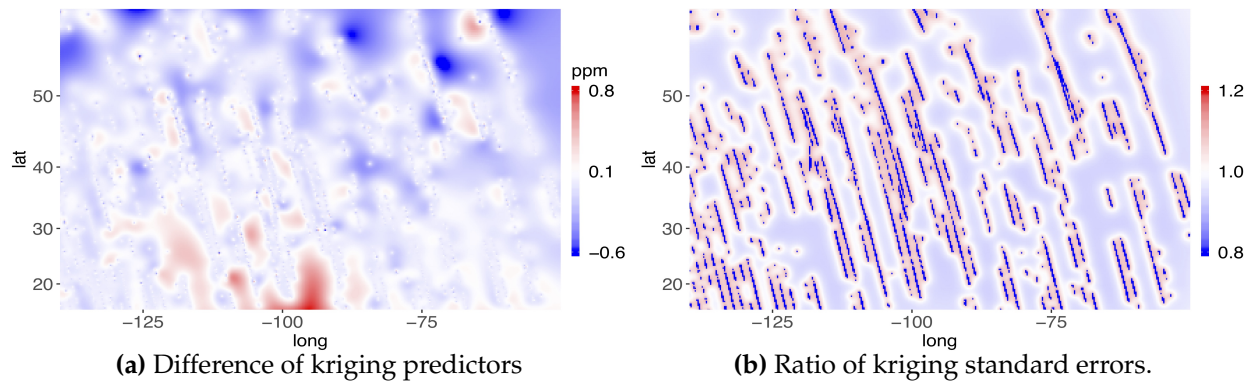


Fig. S.9. Comparison of kriging predictors under the Matérn class and the CH class. The left panel shows the difference between kriging predictors under the CH class and those under the Matérn class. The right panel shows the ratio of kriging standard errors under the CH class to those under the Matérn class.